ANNEX 1:

Contibution to other papers

Pergamon

www.neuroscience-ibro.com

PII: S0306-4522(02)00058-1

Neuroscience Vol. 113, No. 3, pp. 709–719, 2002

0306-4522/02 $22.00+0.00

INTERACTIONS AMONG ADENOSINE DEAMINASE, ADENOSINE A_1 RECEPTORS AND DOPAMINE D_1 RECEPTORS IN STABLY COTRANSFECTED FIBROBLAST CELLS AND NEURONS

M. TORVINEN,[a*] S. GINÉS,[b] J. HILLION,[a] S. LATINI,[c] M. CANALS,[b] F. CIRUELA,[b] F. BORDONI,[c] W. STAINES,[a] F. PEDATA,[c] L. F. AGNATI,[d] C. LLUIS,[b] R. FRANCO,[b] S. FERRÉ[e] and K. FUXE[a]

[a]Department of Neuroscience, Karolinska Institute, 171 77 Stockholm, Sweden

[b]Department of Biochemistry and Molecular Biology, University of Barcelona, 08028 Barcelona, Spain

[c]Department of Preclinical and Clinical Pharmacology, University of Florence, 50134 Florence, Italy

[d]Department of Biomedical Sciences, University of Modena, Modena, Italy

[e]National Institute on Drug Abuse, National Institutes of Health, Baltimore, MD 21224, USA

Abstract—The role of adenosine deaminase in the interactions between adenosine A_1 and dopamine D_1 receptors was studied in a mouse fibroblast cell line stably cotransfected with human D_1 receptor and A_1 receptor cDNAs (A_1D_1 cells). Confocal laser microscopy analysis showed a high degree of adenosine deaminase immunoreactivity on the membrane of the A_1D_1 cells but not of the D_1 cells (only cotransfected with human D_1 receptor cDNAs). In double immunolabelling experiments in A_1D_1 cells and cortical neurons a marked overlap in the distribution of the A_1 receptor and adenosine deaminase immunoreactivities and of the D_1 receptor and adenosine deaminase immunoreactivities was found. Quantitative analysis of A_1D_1 cells showed that adenosine deaminase immunoreactivity to a large extent colocalizes with A_1 and D_1 receptor immunoreactivity, respectively. The A_1 receptor agonist caused in A_1D_1 cells and in cortical neurons coaggregation of A_1 receptors and adenosine deaminase, and of D_1 receptors and adenosine deaminase. The A_1 receptor agonist-induced aggregation was blocked by *R*-deoxycoformycin, an irreversible adenosine deaminase inhibitor. The competitive binding experiments with the D_1 receptor antagonist [^{3}H]SCH-23390 showed that the D_1 receptors had a better fit for two binding sites for dopamine, and treatment with the A_1 receptor agonist produced a disappearance of the high-affinity site for dopamine at the D_1 receptor. *R*-Deoxycoformycin treatment, which has previously been shown to block the interaction between adenosine deaminase and A_1 receptors, and which is crucial for the high-affinity state of the A_1 receptor, also blocked the A_1 receptor agonist-induced loss of high-affinity D_1 receptor binding.

The conclusion of the present studies is that the high-affinity state of the A_1 receptor is essential for the A_1 receptor-mediated antagonistic modulation of D_1 receptors and for the A_1 receptor-induced coaggregates of A_1 and adenosine deaminase, and of D_1 and adenosine deaminase. Thus, the confocal experiments indicate that both A_1 and D_1 receptors form agonist-regulated clusters with adenosine deaminase, where the presence of a structurally intact adenosine deaminase bound to A_1 receptors is important for the A_1–D_1 receptor–receptor interaction at the level of the D_1 receptor recognition.

Key words: adenosine deaminase, adenosine A_1 receptor, dopamine D_1 receptor, fibroblast cell line, neuronal primary cultures, heteromers.

The nucleoside adenosine exerts a modulatory action via its G protein-coupled receptors in many areas of the CNS. The two main metabolic pathways of adenosine removal involve the enzymes adenosine deaminase (ADA) and adenosine kinase. ADA is an enzyme which participates in the purine metabolism where it degrades adenosine to inosine (Fredholm, 1995). ADA is located both in the cytosol and on the cell membrane, and the ecto-form of ADA binds to the plasma membrane via membrane proteins. Two of them have been identified: the T-cell activation marker molecule CD26 and adenosine A_1 receptors (Franco et al., 1997). Adenosine A_1 receptors and ecto-ADA are functionally coupled. Thus, irrespective of its catalytic activity, ADA has been shown to be necessary for the existence of the high-affinity binding state of A_1 receptors and, therefore, for allowing efficient A_1 receptor signal transduction by forming a heteromeric complex (Ciruela et al., 1996; Saura et al., 1996). In a smooth muscle cell line (DDT1MF-2 cells) ADA and A_1 receptors internalize together via the same endocytotic pathway following agonist-induced receptor desensitization, accelerating the

*Corresponding author. Tel.: +46-8-7287090; fax: +46-8-337941.
E-mail address: maria.torvinen@neuro.ki.se (M. Torvinen).

Abbreviations: ADA, adenosine deaminase; CPA, *N*6-cyclopentyladenosine; DCF, *R*-deoxycoformycin; FA, field area; FITC, fluorescein isothiocyanate; GV, gray value; HPLC, high-performance liquid chromatography; K_H, high-affinity binding state; K_L, low-affinity binding state; PBS, phosphate-buffered saline; PTX, pertussis toxin; RGB, red, green, blue; R_H, proportion of receptors in the high-affinity state; *R*-PIA, *R*-phenylisopropyladenosine; SCH-23390, 7-chloro-8-hydroxy-3-methyl-1-phenyl-2,3,4,5-tetrahydro-1*H*-3-benzazepine; SKF-38393, 2,3,4,5-tetrahydro-7,8-dihydroxy-1-phenyl-1*H*-3-benzazepine; TRITC, tetramethylrhodamine isothiocyanate.

ligand-induced A_1 receptor desensitization and internalization (Saura et al., 1998).

There exists a large amount of data showing the existence of antagonistic interactions between adenosine and dopamine receptors in the striatum. Adenosine receptor agonists and antagonists produce behavioral effects similar to dopamine receptor antagonists and agonists, respectively. These interactions seem to be subtype specific, occurring mainly between adenosine A_{2A} and dopamine D_2 receptors in the GABAergic striopallidal neurons and between adenosine A_1 and dopamine D_1 receptors in the strionigral and strioendopeduncular neurons (Ferré et al., 1997). The results from membrane preparations both from rat striatum and from a fibroblast cell line stably cotransfected with A_1 and D_1 receptor cDNAs (A_1D_1 cells) show that stimulation of A_1 receptors decreases the proportion of D_1 receptors in the high-affinity state for agonists (R_H), without modifying the dissociation constants of the high- and low-affinity states (K_H and K_L, respectively) (Ferré et al., 1994, 1998). Finally, by using coimmunoprecipitation and confocal laser microscopy techniques, we have recently shown that A_1 and D_1 receptors form agonist-regulated heteromeric complexes in the A_1D_1 fibroblast cells (Ginés et al., 2000).

In previous experiments pretreatment of A_1D_1 cells with pertussis toxin (PTX) counteracted the effect of low but not high concentrations of the A_1 receptor agonist *N*6-cyclopentyladenosine (CPA) on the binding characteristics of D_1 receptors (Ferré et al., 1998). The main effect of PTX seems to be an uncoupling of the A_1 receptor from its G protein by inducing an ADP ribosylation of the G_α subunit of the G_i (and G_o) protein family. This results in a reduction of the number of A_1 receptors in the high-affinity state and in a blockade of the A_1 receptor signal transduction (Kurose, 1983). It was, therefore, hypothesized that the results obtained with PTX indicated a possible modulatory influence of both states of affinity of A_1 receptors on D_1 receptor binding (Ferré et al., 1998). However, the observed PTX-induced G protein ribosylation was incomplete. Consequently, it was not possible to rule out that the stimulation with the high concentration of CPA of the low number of A_1 receptors left in the high-affinity state after PTX pretreatment could reproduce the same effect as the low concentration of CPA in the absence of PTX pretreatment.

The aim of the present study was to characterize the involvement of ADA in the antagonistic intramembrane interaction between A_1 and D_1 receptors in the A_1D_1 fibroblast cells. ADA, A_1 and D_1 receptors were identified by immunocytochemistry in combination with confocal laser microscopy techniques. Endogenous adenosine measurements and D_1 receptor binding experiments were performed in crude membrane preparations with or without the addition of exogenous adenosine or CPA.

EXPERIMENTAL PROCEDURES

Cell cultures

Previously characterized mouse fibroblast Ltk$^-$ cells transfected with human D_1R cDNA (D_1 cells) and with both human D_1R and human A_1R cDNAs (A_1D_1 cells) were used. The determined B_{max} values for the A_1 and D_1 receptors were 4.0 ± 0.4 and 4.6 ± 0.3 pmol/mg protein, respectively (means ± S.E.M.) (Ferré et al., 1998). Ltk$^-$ cells were grown as previously described (Ferré et al., 1998). For primary cultures of neurons cerebral cortices were taken out from 17–18-day-old Sprague–Dawley rat embryos (B&K Universal, Sweden) in Ca^{2+} and Mg^{2+} free phosphate buffer (PBS Dulbecco's, Gibco, Sweden) supplemented with 6 mg/ml glucose, and 20 U/ml penicillin and 20 µg/ml streptomycin (Gibco). The experiments were approved by the local ethical committee (Stockholms norra Försöksdjurs Etiska Kommittee), and care was taken to minimize the number of animals used and to minimize any suffering. The tissue fragments were pooled and mechanically dissociated in culture medium. The culture medium consisted of Eagle's basal medium (Gibco) supplemented with 10% fetal bovine serum (Gibco), 25 mM KCl (Merck, Sweden), 2 mM glutamine (Sigma, Sweden) and 100 µg/ml gentamicin (Sigma). Cells were collected by centrifugation at $100 \times g$ for 5 min and resuspended in fresh medium. The resulting single cell suspension was seeded at a density of about 5×10^5 cells/well on gelatin (250 µg/ml in 15 mM borate buffer, pH 8.4, Sigma)–poly-L-lysine (10 µg/ml, Sigma)-coated 24-well plates (Falcon, Sweden) in the same medium. The cells were grown at 37°C in saturation humidity in a 5% CO_2–95% air atmosphere for 6 days.

Immunostaining experiments

For immunofluorescence staining, transfected cells (A_1D_1 and D_1) or primary cultures of cortical neurons growing on glass coverslips were incubated in the absence or presence of the adenosine A_1 receptor agonist *R*-phenylisopropyladenosine (*R*-PIA; 100 nM) or the dopamine D_1 receptor agonist SKF-38393 (2,3,4,5-tetrahydro-7,8-dihydroxy-1-phenyl-1*H*-3-benzazepine; 10 µM) and/or the irreversible ADA inhibitor *R*-deoxycoformicin (DCF, 0.1 µM) in serum free medium for 1 h at 37°C. They were rinsed in phosphate-buffered saline (PBS) and fixed in 4% paraformaldehyde in PBS for 15 min and washed in PBS containing 20 mM glycine. For permeabilization, an additional incubation (7 min) with 0.01% saponin (transfected cells) or 0.2% Triton X-100 (cortical neurons) in PBS was performed. Cells were subsequently treated with PBS–20 mM glycine–1% bovine serum albumin for 30 min at room temperature. Double immunostaining was performed with fluorescein isothiocyanate-conjugated polyclonal anti-ADA antibody (anti-ADA–FITC, 40 µg/ml) (Ciruela et al., 1996) and tetramethylrhodamine isothiocyanate-conjugated polyclonal anti-A_1 receptor antibody (PC21–TRITC, 20 µg/ml for transfected cells or 50 µg/ml for cortical neurons) (Ginés et al., 2000) or Texas Red-conjugated anti-D_1 receptor antibody (D1-356-446-Tx, 5 µg/ml for transfected cells or 10 µg/ml for cortical neurons) (Bjelke et al., 1996) for 1 h at 37°C. The coverslips were rinsed for 40 min in the same buffer and mounted with medium for immunofluorescence (ICN Biomedicals, Costa Mesa, USA). In a control experiment the specificity of the labelling was tested as a lack of specific immunofluorescence in a double immunostaining experiment performed as described above with the same amount of rabbit IgG–TRITC and rabbit IgG–FITC. For each treatment two coverslips (duplicates) containing more than 500 000 cells were studied and more than 15 fields (randomly selected) were analyzed on each coverslip. No differences between fields were found and a representative cell or cells are shown. Confocal microscope observations were made with a Leica TCS 4D (Leica Lasertechnik, Heidelberg, Germany) confocal scanning laser equipment adapted to an inverted Leitz DMIRBE microscope. In all cases, images represent a horizontal section of cells. The quantitative analysis of % colocalization was performed with a Zeiss KS400 Imaging System.

Image analysis

The image analysis KS400 system was used for the quantita-

tive analysis of the immunolabelling experiments. After acquisition of the images the discrimination procedure based on the function 'Threshold RGB' (red, green, blue) was used. A suitable threshold has been interactively selected for the red (visualization of the receptors) or green (visualization of the ADA enzyme) fluorophores in such a way that the profiles of the cells could be detected in their entirety. This threshold was found to be mean gray value (GV) 100 and the corresponding field area (FA) was measured (basal FA). Then successive thresholds (GV thresholds for R and G) have been employed to discriminate the most intense area of emission (Agnati and Fuxe, 1974). For each of these thresholds the respective FAs have been measured and then expressed as percentages of the respective FA basal value for ADA. By means of the Boolean operator 'AND' the overlap area (that is the colocalization area) of the receptor (A_1 or D_1) and ADA staining was evaluated at each threshold value (see Table 1).

Adenosine measurements

Samples were analyzed from the different membrane preparations obtained after preincubation (30 min) with or without DCF (0.1 μM). Adenosine content was analyzed by high-performance liquid chromatography (HPLC) coupled to a spectrofluorimetric detector, as previously described (Latini et al., 1998; Melani et al., 1999; Wojcik and Neff, 1982). In order to purify samples and adenosine standards (prepared in the same volume of incubation buffer) from salts, they were freeze-dried overnight, resuspended in 1 ml of methanol and centrifuged at 1200×*g* for 20 min at 4°C. The supernatant was evaporated under nitrogen and resuspended in 110 μl of zinc acetate (0.05 M). Since adenosine was detected as a fluorescent derivative (1,*N*6-ethenoadenosine) following derivatization with chloroacetaldehyde, the solution was transferred into glass vials, where 0.18 μl of chloroacetaldehyde (4.5%) was added for each μl of solution obtained. Samples were kept for 20 min at 100°C, and 100 μl of this solution was injected for HPLC analysis utilizing a nucleosil C-18 column (inner diameter: 4.6 mm; length: 150 mm; Waters, MA, USA) with a particle size of 3.5 μm. The mobile phase used to resolve adenosine was an acetate buffer (50 mM, pH 5) with 5% acetonitrile (v/v) and 1 mM l-octanesulfonic acid sodium salt (Eastman Kodak, Rochester, NY, USA) which ran at a flow rate of 0.8 ml/min. To protect the system from clogging with particulate matter, a Waters In-Line filter with 2-μm pore size was incorporated into the HPLC system upstream from the stationary phase column. To detect adenosine the spectrofluorimetric detector (LC-240, Perkin Elmer, Norwalk, CT, USA) was utilized with a fixed excitation wavelength set at 270 nm and a fixed emission wavelength set at 394 nm. The adenosine peaks were identified and quantified by comparing retention time and peak heights with those of known standards run according to the sample procedure. Adenosine was also identified by its disappearance after incubation of the sample with 1 U of ADA at room temperature for 1 min. The minimal detectable amount of adenosine was 0.1 pmol.

Membrane preparations for radioligand binding experiments

The cells were lifted from Petri dishes with a cell scraper. Harvested cells were washed twice with ice-cold PBS and centrifuged at 1200×*g* for 5 min at 4°C. The cell pellet was sonicated (30 s) and resuspended in the incubation buffer in the absence or presence of ADA (Boehringer Mannheim; 5 U/ml) or the irreversible ADA inhibitor DCF (0.1 μM). The homogenate was centrifuged at 1800×*g* for 10 min at 4°C, the precipitated nuclear fraction was discarded and the supernatant was preincubated for 30 min at 37°C or at room temperature and centrifuged at 40 000×*g* for 40 min at 4°C. The membrane pellet was then resuspended by sonication in the incubation buffer: 50 mM Tris–HCl (pH 7.4) containing 120 mM $NaCl_2$, 5 mM KCl, 2 mM $CaCl_2$ and 1 mM $MgCl_2$. Preincubation with DCF (0.1 μM) was performed under the same conditions as for the determination of the concentration of adenosine (room temperature). This inhibitor, at the concentration used, completely inhibits ADA activity at room temperature (unpublished data).

Radioligand binding experiments

Competition experiments of dopamine (1 nM–10 mM) versus D_1 receptor antagonist [^{3}H]SCH-23390 (7-chloro-8-hydroxy-3-methyl-1-phenyl-2,3,4,5-tetrahydro-1*H*-3-benzazepine; 70.3 Ci/mmol) (∼2 nM) were performed by incubation for 15 min at 37°C in the presence or absence of the adenosine A_1 receptor agonist CPA (10 nM or 10 μM) or adenosine (1 μM) (final protein concentration 0.2 mg/ml). The incubation was stopped by fast filtration through glass-fiber filters (GF/B, Whatman) by washing three times with 5 ml of 50 mM ice-cold Tris–HCl (pH 7.4) with an automatic cell harvester (Brandel). The radioactivity content of the filters was detected by liquid scintillation spectrometry. Data from competition experiments were analyzed by non-linear regression analysis, and the fitting for either one or two binding sites was statistically compared (*F* test). For a two-binding site fit, dissociation constants for the high- (K_H) and low-affinity (K_L) binding sites and for the proportion of binding sites in the high-affinity state (R_H) were analyzed. For one binding site fit, the concentration of agonist that displaced 50% of the labelled antagonist (IC_{50}) was determined.

RESULTS

Identification of ADA in D_1 and A_1D_1 cells

A high degree of ADA immunoreactivity was detected on the plasma membrane in non-permeabilized A_1D_1 cells but not on the plasma membrane in non-permeabilized D_1 cells (Fig. 1). After permeabilization, however, ADA immunoreactivity was demonstrated in the D_1 cells due to its location in the cytoplasm (Fig. 1).

Table 1. FAs expressed as percentage of the respective ADA basal value

	GV threshold 100 mean (±S.E.M.)	GV threshold 150 mean (±S.E.M.)	GV threshold 200 mean (±S.E.M.)
A_1	134 (±10)	84 (±15)	36 (±7)
ADA	100 (±8)	42 (±6)	4 (±6)
A_1/ADA	96 (±8)	36 (±5)	3 (±5)
D_1	148 (±12)	68 (±11)	13 (±6)
ADA	100 (±7)	39 (±6)	3 (±5)
D_1/ADA	93 (±8)	32 (±7)	1 (±4)

As explained in Experimental procedures different thresholds for the intensity of emission for red (corresponds to rhodamine-conjugated anti-A_1 or Texas Red-conjugated anti-D_1 antibodies) and green (corresponds to fluorescence-conjugated anti-ADA antibodies) fluorescence have been selected and the corresponding FAs measured. By means of the Boolean operator 'AND' the overlap areas between ADA and A_1 receptor immunoreactivities and ADA and D_1 receptor immunoreactivities have been evaluated at the different thresholds of fluorescence intensities. Image analysis of colocalization of A_1/ADA and D_1/ADA immunoreactivity in A_1/D_1-transfected Ltk fibroblast cells in the basal state (sample size, $n = 3$).

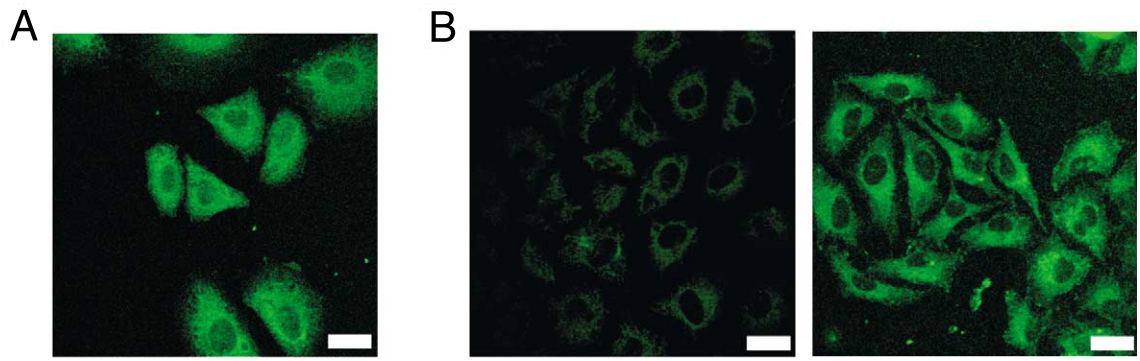

Fig. 1. Expression of ADA in A_1D_1 cells and D_1 cells. Transfected cells were processed for immunostaining (see Experimental procedures) using fluorescein-conjugated anti-ADA antibody. The cells were analyzed by confocal microscopy. (A) ADA immunoreactivity in non-permeabilized A_1D_1 cells. (B) Absence of ADA immunoreactivity in non-permeabilized (left) and presence of ADA immunoreactivity in permeabilized (right) D_1 cells. Scale bars = 50 μm.

Double immunolabelling experiments in A_1D_1 cells

As previously described (Ginés et al., 2000) a high degree of A_1 and D_1 receptor immunoreactivities was found in the A_1D_1 fibroblast cells. With the confocal laser microscopy it was possible to see a homogenous distribution of A_1 receptors and D_1 receptors in the A_1D_1 cells (Fig. 2). It should be noted that the anti-D_1 antibody used is directed against a cytoplasmic region of the receptor. Therefore, all immunolocalizations requiring anti-D_1 antibody were performed in permeabilized cells. In double immunolabelling experiments, the analysis of these cells showed a marked overlap in the distribution of the A_1 receptor and ADA (Fig. 2A), and of the D_1 receptor and ADA (Fig. 2B). Computer-assisted image analysis demonstrated that ADA immunoreactivity to a large extent colocalizes with A_1 and D_1 receptor immunoreactivity, respectively (Table 1). How-

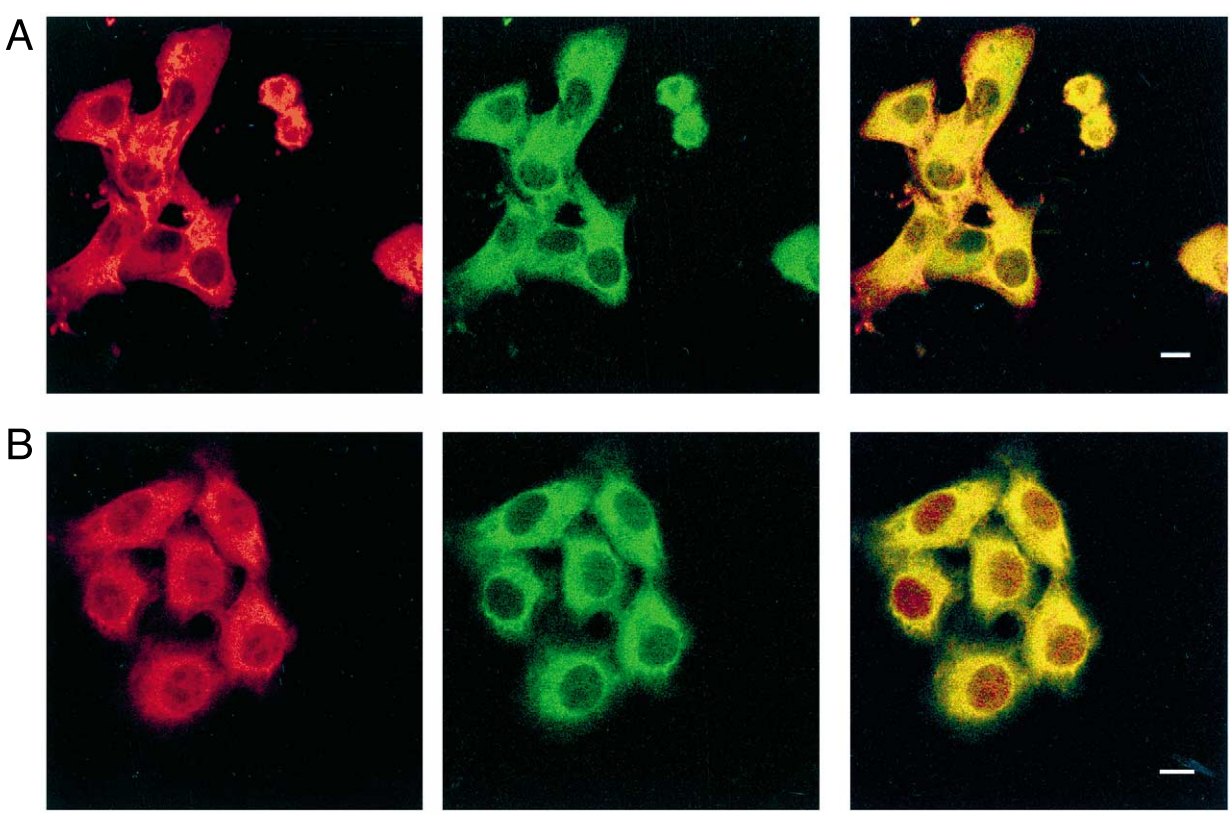

Fig. 2. ADA, adenosine A_1 receptor and dopamine D_1 receptor distributions in permeabilized A_1D_1 cells. Transfected cells were processed for immunostaining (see Experimental procedures) using fluorescein-conjugated anti-ADA and rhodamine-conjugated anti-A_1 receptor antibodies (A) or fluorescein-conjugated anti-ADA and Texas Red-conjugated anti-D_1 receptor antibodies (B). The cells were analyzed by confocal microscopy. Superimposition of images reveals the colocalization of ADA and A_1 receptor (image on the right in A), and of ADA and D_1 receptor immunoreactivities (image on the right in B) in yellow. Scale bars = 10 μm.

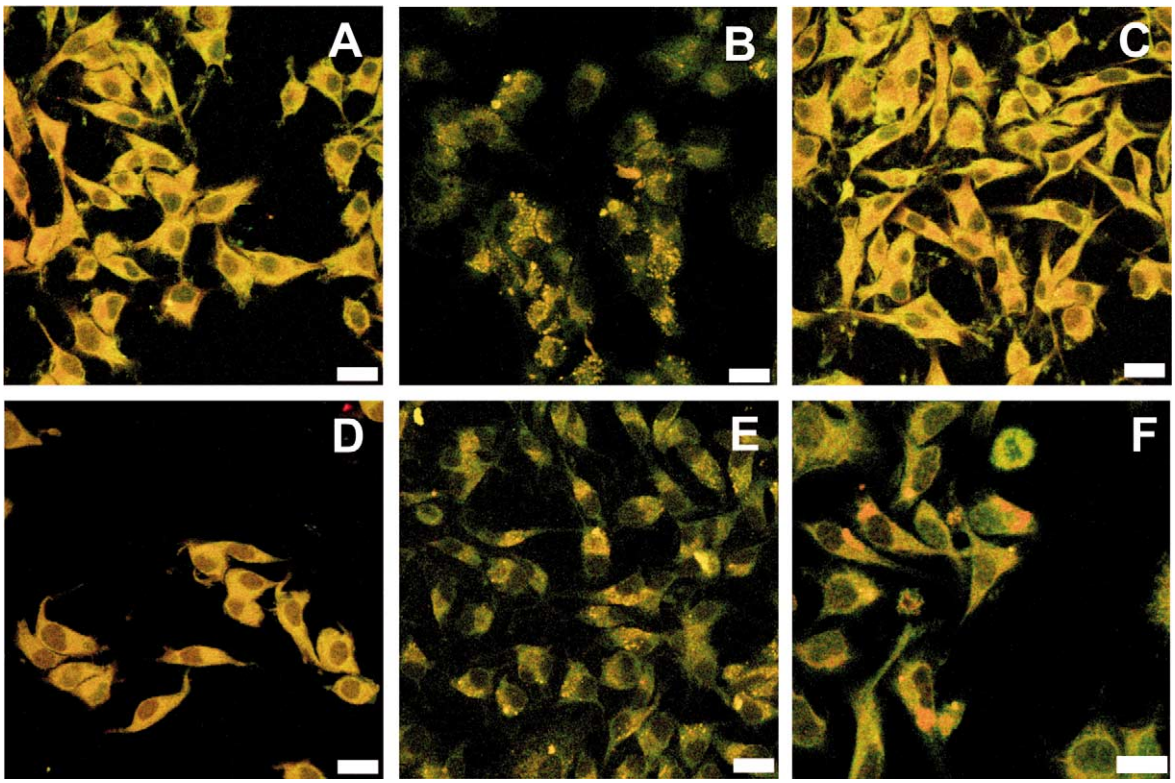

Fig. 3. Effects of the ligands on ADA colocalization with A_1 adenosine receptors and with D_1 receptors. A_1D_1 cells were incubated for 1 h in the medium in the absence (A and D) or presence of 100 nM A_1 receptor agonist *R*-PIA (B and E) or in the presence of 10 μM dopamine D_1 receptor agonist SKF-38393 (C and F). Cells were processed for immunostaining as indicated in the legend of Fig. 2 and were analyzed by confocal microscopy. Only the colocalization (in yellow) between ADA and adenosine A_1 receptor (A–C), and between ADA and dopamine D_1 receptor (D–F) immunoreactivities is shown. Scale bars = 50 μm.

ever, a small part of both A_1 and D_1 receptor immunoreactivity did not colocalize with ADA immunoreactivity (Table 1). When the cells were treated for 1 h with the A_1 receptor agonist *R*-PIA (100 nM), a redistribution of the A_1 receptor and ADA immunoreactivity was observed (Fig. 3B). Thus, *R*-PIA induced the aggregation of both proteins in clusters seen as a punctate fluorescence with a high degree of colocalization of A_1 receptors and ADA (Fig. 3B). In contrast, the D_1 receptor agonist SKF-38393 (10 μM) did not modify the A_1 receptor or the ADA immunoreactivity nor the A_1 receptor/ADA colocalization (Fig. 3C). In double D_1 receptor/ADA immunolabelling experiments pretreatment with the A_1 agonist also induced aggregation (clusters) of D_1 receptors and ADA (punctate fluorescent regions) with a high degree of colocalization between D_1 receptors and ADA (Fig. 3E). However, the D_1 receptor agonist only induced clustering of D_1 receptors resulting in a loss of the D_1 receptor/ADA colocalization (Fig. 3F).

The presence of the ADA inhibitor DCF alone did not modify the colocalization of ADA/A_1 and ADA/D_1 (results not shown). Fig. 4 shows the effect of DCF on the *R*-PIA-induced clustering of ADA/A_1 and ADA/D_1. As shown in Fig. 4A, in the presence of DCF the A_1 receptor agonist is not able to induce the A_1/ADA aggregation seen in the absence of DCF (see Fig. 3B) nor the D_1/ADA aggregation (compare Fig. 4B with Fig. 3E).

Double immunolabelling experiments in primary rat cortical neurons

As seen in Fig. 5, the cultured neurons showed A_1 receptor, D_1 receptor and ADA immunoreactivities. The location of both receptors and ADA was diffuse in the soma and dendrites with a high degree of A_1 receptor/ADA colocalization (Fig. 5A) and of D_1 receptor/ADA colocalization (Fig. 5B). The degree of A_1 receptor/ADA colocalization analyzed with an image analysis system was similar to that found in cotransfected fibroblast cells while in contrast to the fibroblast cells part of ADA immunoreactivity was not fully associated with D_1 receptor immunoreactivity probably related to the overexpression of D_1 receptors (4.6 ± 0.3 pmol/mg protein; mean ± S.E.M.) in the fibroblast cells (data not shown for simplicity, see Fig. 5B). The A_1 receptor agonist *R*-PIA (100 nM) induced a coaggregation of A_1 receptor and ADA and of D_1 receptor and ADA (Fig. 5A, B) in the cortical neurons. This was also true for the D_1 receptor agonist SKF-38393 (10 μM) (Fig. 5A, B).

Adenosine concentration in D_1 and A_1D_1 cells

Endogenous ADA was found to be very active in membrane preparations from both D_1 and A_1D_1 cells, since preincubation with the irreversible ADA inhibitor

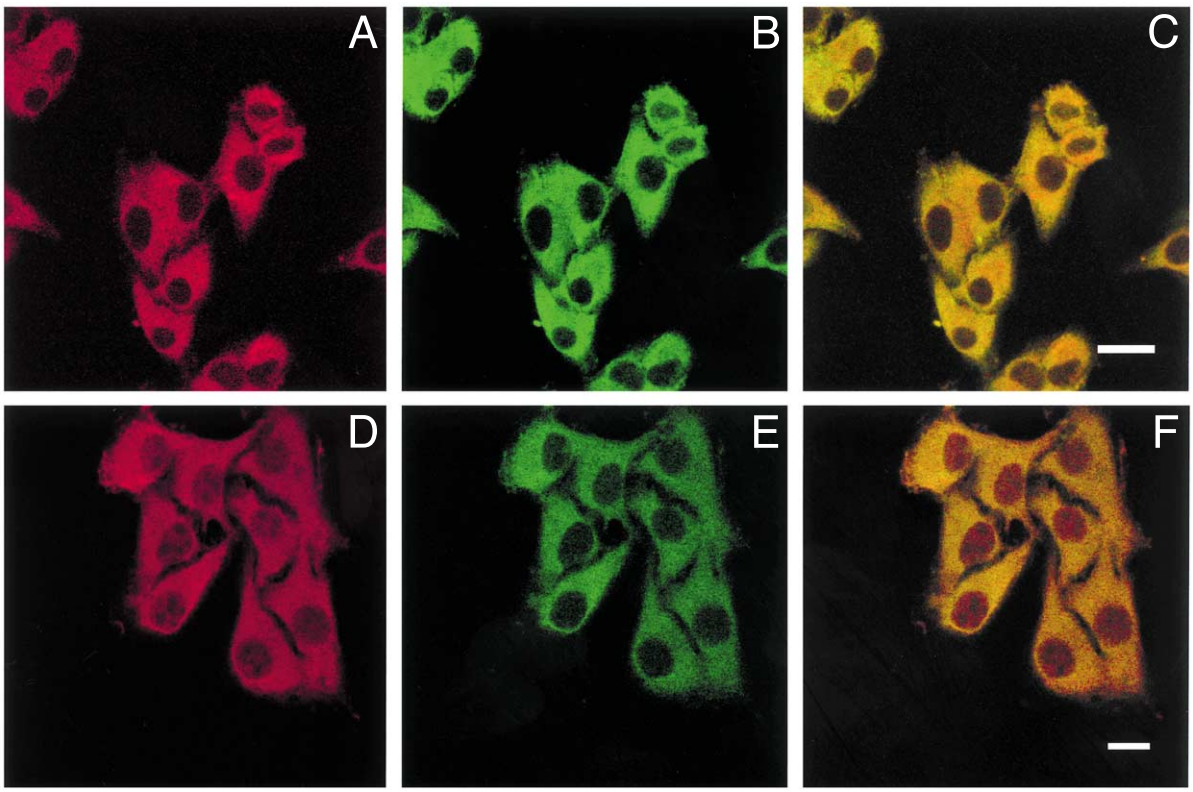

Fig. 4. Effects of *R*-PIA on ADA colocalization with A_1 adenosine receptors and with D_1 receptors in the presence of DCF. A_1D_1 cells were incubated for 1 h with 100 nM A_1 receptor agonist *R*-PIA and 0.1 μM of the irreversible ADA inhibitor DCF. Cells were processed for immunostaining (see Experimental procedures) using fluorescein-conjugated anti-ADA and rhodamine-conjugated anti-A_1 receptor antibodies (A–C) or fluorescein-conjugated anti-ADA and Texas Red-conjugated anti-D_1 receptor antibodies (D–F). The cells were analyzed by confocal microscopy. Superimposition of images corresponding to ADA staining (A) and A_1 receptor staining (B) reveals the colocalization of ADA and A_1 receptor immunoreactivities in yellow (C). Superimposition of images corresponding to ADA staining (D) and D_1 receptor staining (E) reveals the colocalization of ADA and D_1 receptor immunoreactivities in yellow (F). The effect of 100 nM *R*-PIA in the absence of DCF is shown in Fig. 3B, E. Scale bars = 10 μm.

DCF (0.1 μM) induced a large increase (about 10 times) in the concentration of adenosine in both cell lines (Table 2). Furthermore, a decrease of about 10 times in the concentration of exogenously added adenosine (1 μM) was obtained after incubation for 15 min at 37°C (the median of the final concentration was 0.075 μM, with an interquartile range of 0.022 μM). The concentration of adenosine present in the membrane preparations after preincubation at 37°C was significantly lower than that obtained after preincubation at room temperature. This suggests that the effect of endogenous ADA is enhanced at 37°C (the optimal temperature for the enzymatic effect of ADA). Similar adenosine concentrations were observed in membrane preparations from D_1 and A_1D_1 cells for the different preincubation protocols (Table 2).

Role of ADA in the modulation of the binding characteristics of D_1 receptors

In competitive inhibition curves of dopamine versus the D_1 receptor antagonist [^{3}H]SCH-23390, a best fitting for two binding sites was obtained in membrane preparations from D_1 cells (Table 3). A best fitting for two binding sites with similar K_H, K_L and R_H values to these previously obtained by Ferré et al. (1998) was also present in the membrane preparations from the A_1D_1 cells (Table 3). CPA (10 nM) or adenosine (1 μM) produced a disappearance of R_H (significantly best fitting for one binding site) in membrane preparations from A_1D_1 cells (Table 3). The final concentration of exogenously added adenosine in the incubation buffer was 0.075 μM

Table 2. Concentration of adenosine in membrane preparations from D_1 and A_1D_1 cells

Preincubation protocol	Adenosine (μM)
D_1 cells	
Room temperature	0.024 (0.014)
37°C	0.009 (0.008)*
DCF	0.424 (0.256)**
A_1D_1 cells	
Room temperature	0.029 (0.016)
37°C	0.009 (0.007)**
DCF	0.314 (0.207)**

Results are expressed as medians and the interquartile ranges are given in parentheses ($n = 5$–8/experiment). Preincubation with DCF (0.1 μM) was performed at room temperature. * and ** $P < 0.05$ and $P < 0.01$ compared to the group with preincubation at room temperature (Kruskal–Wallis test, followed by post-hoc Mann–Whitney's *U* test) ($n = 5$–8/group).

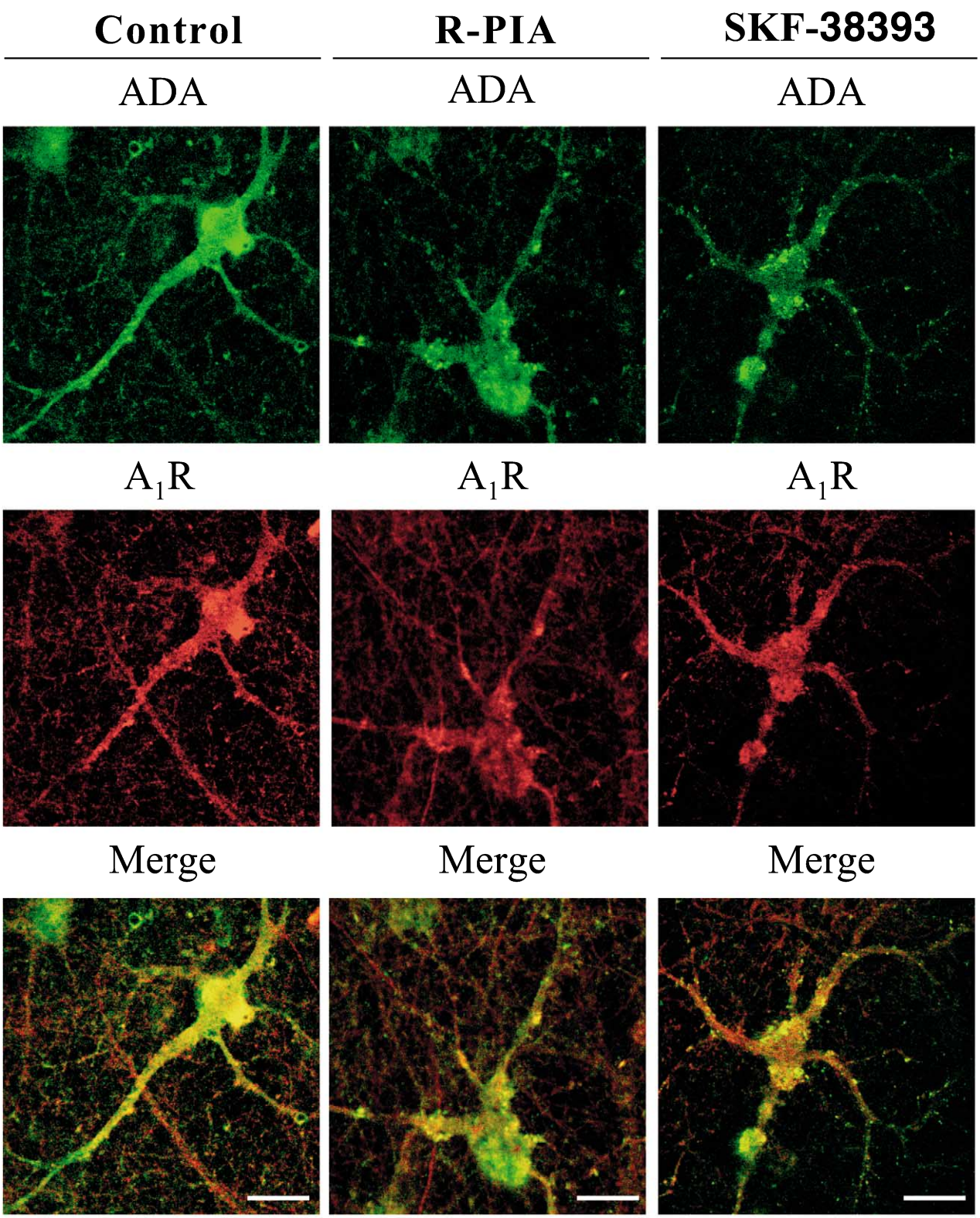

Fig. 5 (*Caption overleaf*).

B

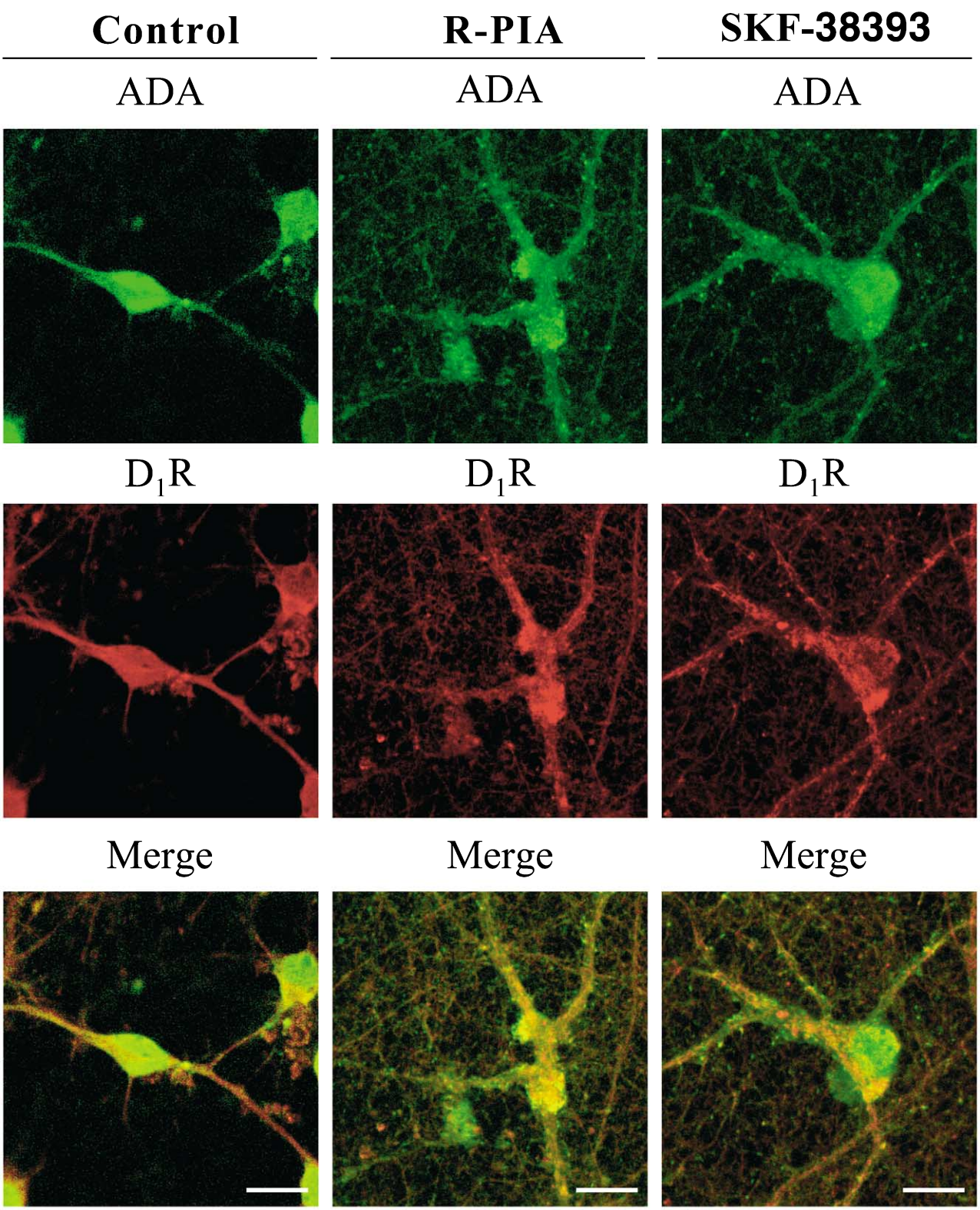

Fig. 5. Effects of agonists on adenosine A_1 receptors and ADA (A), and dopamine D_1 receptors and ADA (B) in primary cultures of cortical neurons. The primary cultures were incubated for 1 h with medium in the absence (control) or presence of the A_1 agonist *R*-PIA (100 nM) or the dopamine D_1 receptor agonist SKF-38393 (10 μM) and were processed for immunostaining (see Experimental procedures) using fluorescein-conjugated anti-ADA (ADA) and Texas Red-conjugated anti-A_1 (A_1R) and anti-D_1 (D_1R) antibodies. The primary cultures of cortical neurons on coverslips were analyzed by confocal microscopy. Superimposition of images (Merge) reveals the colocalization of A_1 receptor/ADA and D_1 receptor/ADA immunoreactivities. Scale bars = 10 μm.

(see above). Finally, preincubation with DCF completely counteracted the disappearance of the R_H at the D_1 receptors induced by the adenosine A_1 agonist CPA (10 nM and 10 μM) in A_1D_1 cells (Table 3) in spite of its ability to substantially increase adenosine levels (Table 2) in the membrane preparations. These findings can be explained by an uncoupling of the A_1 receptor/ADA complex (see Fig. 4A) by DCF and are in line with previous findings (Saura et al., 1996).

DISCUSSION

The role of ADA in the A_1/D_1 interaction

In experiments dealing with adenosine A_1 receptors, ADA is routinely added to metabolize endogenous adenosine, which would otherwise interfere with the binding of exogenous ligands to the A_1 receptor. However, previous work has demonstrated that ADA also plays an essential role in the function of A_1 receptor (Franco et al., 1997). Adenosine A_1 receptors (and other cell surface receptors, such as CD26) bind ADA, which in this way can act as an ecto-enzyme (Franco et al., 1997), and form heteromeric complexes with A_1 receptors (Ginés et al., 2000). ADA, independently of its enzymatic activity, is necessary for the existence of the high-affinity binding state of A_1 receptors and, thus, for efficient A_1 receptor signal transduction. Furthermore, ADA is involved in the ligand-induced A_1 receptor desensitization (Saura et al., 1996, 1998). In membrane preparations from rat striatum and from Ltk cells stably cotransfected with A_1 and D_1 receptor cDNAs, stimulation of A_1 receptors decreases the proportion of D_1 receptors in the high-affinity state (Ferré et al., 1998). Therefore, it becomes important to determine the association of ADA with the A_1/D_1 heteromers and the role of ADA in the A_1 receptor-mediated modulation of the binding characteristics of D_1 receptors.

The activity of endogenous ADA

The immunostaining experiments showed that ADA could only be detected in the plasma membrane of A_1D_1 cells. However, in permeabilized cells (A_1D_1 or D_1 cells) ADA immunoreactivity was also found in the cytoplasm. Therefore, these results give further evidence that ADA depends on anchoring proteins, such as A_1 receptors, to be localized to the plasma membrane (Franco et al., 1997). The activity of endogenous ADA was established by measuring the concentration of adenosine in membrane preparations from D_1 and A_1D_1 cells under different preincubation protocols. Although differently to A_1D_1 cells, non-permeabilized D_1 cells did not show any ADA immunoreactivity, the same adenosine concentrations were observed in membrane preparations from both kinds of cotransfected cells. This suggests that ecto-ADA contributes very little to the total ADA enzymatic activity found in crude membrane preparations from A_1D_1 cells. The irreversible ADA inhibitor DCF induced an important increase in adenosine concentration. However, addition of exogenous ADA (results not shown for simplicity) or preincubation at 37°C (the optimal temperature for the enzymatic effect of ADA) significantly reduced adenosine concentration in comparison with the results obtained by preincubation at room temperature. Furthermore, 15 min incubation in 37°C with 1 μM adenosine gave a final adenosine concentration of 75 nM analyzed by HPLC. Altogether these results show that in crude membrane preparations from Ltk cells endogenous ADA has a strong activity, and, therefore, the addition of exogenous ADA is not required. In fact, the A_1 receptor-mediated modulation of D_1 receptor binding characteristics (decrease in R_H values induced by the A_1 receptor agonist CPA or adenosine) was demonstrated in membrane preparations from A_1D_1 cells without addition of exogenous ADA.

The high-affinity state of A_1 receptors is essential for the A_1/D_1 interaction

DCF, by disrupting the A_1 receptor–ADA interaction, has been shown to induce a selective disappearance of the high-affinity state of A_1 receptors (Saura et al., 1996). The loss of ADA enzyme activity caused by DCF is not involved in this action since the marked rise of adenosine

Table 3. Competition–inhibition experiments of dopamine versus the dopamine D_1 receptor antagonist [^{3}H]SCH-23390 in membrane preparations from D_1 and A_1D_1 cells

Treatment	K_H (μM)	K_L/IC_{50} (μM)	R_H (%)
D_1 cells			
Control	0.2 (1.0)	57.4 (23.8)	14.6 (8.4)
ADA preincubation	0.6 (0.8)	55.4 (18.9)	13.1 (6.7)
A_1D_1 cells (without ADA preincubation)			
Control	0.9 (1.3)	67.0 (14.7)	10.5 (5.7)
CPA 10 nM	–	56.0 (12.5)	–
Adenosine 1 μM	–	58.6 (8.5)	–
A_1D_1 cells (DCF preincubation)			
Control	0.3 (0.6)	48.8 (8.4)	12.4 (5.1)
CPA 10 nM	0.3 (1.5)	51.1 (28.7)	12.9 (3.9)
CPA 10 μM	0.3 (0.3)	52.7 (12.5)	11.3 (2.2)

K_H, K_L/IC_{50} and R_H values are expressed as medians and the interquartile ranges are given in parentheses ($n = 4$–12/experiment). Preincubation of membranes from D_1 cells with or without ADA (10 U/ml) and from A_1D_1 cells without ADA was performed at 37°C; preincubation with DCF (0.1 μM) was performed at room temperature.

levels by DCF (to 0.3–0.4 μM) did not cause a reduction of the proportion of D_1 receptors in a high-affinity state for dopamine (R_H). It has previously been shown that Hg^{2+}-inactivated ADA blocks enzyme activity without interfering with the ADA/A_1 interaction or with the high-affinity state of the A_1 receptor (Saura et al., 1996). Thus, the ability of DCF to fully counteract the effects of low and high concentrations of CPA (concentrations which stimulate the high- and low-affinity states of the A_1 receptors, respectively; see Ferré et al., 1998) on the binding characteristics of D_1 receptors strongly suggests that only the high-affinity state of the A_1 receptor is responsible for the A_1 receptor/D_1 receptor at the D_1 recognition level. The affinity of adenosine for the high- and low-affinity states of the cloned human adenosine A_1 receptor (used in the present experiments) has recently been calculated to be around 15 nM and 7 μM, respectively (Cohen et al., 1996). In the experiments described here the concentration of adenosine in the incubation buffer was around 10 nM, which means that the A_1 receptors in the high-affinity state are partially occupied (about 40%) by endogenous adenosine. Since, under these conditions, CPA and adenosine (1 μM added adenosine, which gave a final concentration of 75 nM) were able to modulate the binding characteristics of D_1 receptors, stimulation of the remaining A_1 receptors with a high-affinity state seemed to be necessary to influence D_1 receptor binding characteristics (loss of R_H values). The present results suggest that ADA, by providing the high-affinity state of the A_1 receptor, is essential for the adenosine-mediated modulation of the binding characteristics of D_1 receptors, probably leading to an uncoupling of the D_1 receptors.

Agonists induce clustering of ADA/A_1/D_1 complexes

In agreement with the possible existence of ADA/A_1 receptor/D_1 receptor heteromeric complexes, A_1 and D_1 receptors were found to colocalize with ADA in the A_1D_1 cells and in cortical neurons. A_1 receptor/D_1 receptor colocalization and coimmunoprecipitation have recently been demonstrated in the same cell line (Ginés et al., 2000). ADA seems always to be colocalized with A_1 and D_1 receptors, whereas parts of the A_1 and D_1 receptor populations are not colocalized with ADA (Table 1).

Previous results obtained in the A_1D_1 cotransfected cells showed that 1 h of exposure to A_1 receptor and D_1 receptor agonists had marked effects on the aggregation (clusters) of A_1 and D_1 receptors. Exposure to the A_1 receptor agonist *R*-PIA has been shown to induce a formation of coclusters (coaggregations) containing both A_1 and D_1 receptor immunoreactivities. In contrast, the D_1 receptor agonist SKF-38393 has been shown to disrupt the A_1 receptor/D_1 receptor heteromeric complex, and induce selective aggregation (clustering) of D_1 receptors (Ginés et al., 2000). The results obtained here using double immunolabelling experiments after pretreatment with A_1 or D_1 receptor agonists are in full agreement with these results and support also the existence of ADA/A_1 receptor/D_1 receptor heteromeric complexes. Thus, pretreatment with the A_1 receptor agonist induced clustering of the two complexes formed by ADA/A_1 and ADA/D_1, respectively, which was blocked by DCF. DCF disrupts the ADA/A_1 heteromeric complex and thus prevents the high-affinity state of A_1 receptors. Therefore, the present evidence indicates that A_1 receptor high-affinity state is a prerequisite also for A_1/ADA and D_1/ADA aggregates (clusters). DCF does not disrupt the ADA/A_1 and ADA/D_1 colocalization in the basal state where the high-affinity state of A_1 receptors may not be essential. The relevance of this colocalization is, however, unclear in view of the homogenous distribution of ADA in the cytoplasm and membrane that makes an unspecific colocalization possible and could in fact take place with a number of cytosolic or membrane markers. However, pretreatment of the A_1D_1 cells with the D_1 receptor agonist caused aggregation (clustering) of D_1 receptors with the loss of the D_1 receptor colocalization with A_1 receptors (Ginés et al., 2000) and with ADA (this paper) in agreement with its disruption of the A_1/D_1 heteromeric complex. In contrast, as stated above, the A_1 receptor agonist induces coaggregation of A_1 and D_1 receptors with a postulated cointernalization.

The results obtained from the double immunolabelling experiments in primary cultures of neurons from rat cerebral cortex strongly support the existence of ADA/A_1 receptor/D_1 receptor heteromeric complexes also in neurons. Previous results have shown the existence of colocalization of A_1 and D_1 receptors in these primary cultures (Ginés et al., 2000). In agreement, in the present work a high degree of ADA/D_1 receptor and ADA/A_1 receptor colocalization was found in cortical neurons in culture. Thus, it seems possible that functional heteromeric ADA/A_1 receptor/D_1 receptor complexes also exist in cortical neurons and that their aggregation can be modulated by both dopamine and adenosine as indicated in the present experiments with A_1 and D_1 receptor agonists.

Acknowledgements—Work supported by grants from the Swedish Medical Research Council, the Spanish CICYT (BIO99-0601-C02 and PB97-0984) and 1999–2000 MURST ex 40%, Italy.

REFERENCES

Agnati, L.F., Fuxe, K., 1974. Quantitative comparisons of amine fluorescence in cortical noradrenaline terminals using smear preparations. J. Histochem. Cytochem. 22, 1122–1127.

Bjelke, B., Goldstein, M., Tinner, B., Andersson, C., Sesack, S.R., Steinbusch, H.W., Lew, J.Y., He, X., Watson, S., Tengroth, B., Fuxe, K., 1996. Dopaminergic transmission in the rat retina: evidence for volume transmission. J. Chem. Neuroanat. 12, 37–50.

Ciruela, F., Saura, C., Canela, E.I., Mallol, J., Lluis, C., Franco, R., 1996. Adenosine deaminase affects ligand-induced signalling by interacting with cell surface adenosine receptors. FEBS Lett. 380, 219–223.

Cohen, F.R., Lazareno, S., Birdsall, N.J.M., 1996. The affinity of adenosine for the high- and low-affinity states of the human adenosine A1 receptor. Eur. J. Pharmacol. 309, 111–114.
Ferré, S., Fredholm, B.B., Morelli, M., Popoli, P., Fuxe, K., 1997. Adenosine-dopamine receptor–receptor interactions as an integrative mechanism in the basal ganglia. Trends Neurosci. 20, 482–487.
Ferré, S., Popoli, P., Giménez-Llort, L., Finnman, U.B., Martínez, E., Scotti de Carolis, A., Fuxe, K., 1994. Postsynaptic antagonistic interaction between adenosine A1 and dopamine D1 receptors. NeuroReport 6, 73–76.
Ferré, S., Torvinen, M., Antoniou, K., Irenius, E., Civelli, O., Arenas, E., Fredholm, B.B., Fuxe, K., 1998. Adenosine A1 receptor-mediated modulation of dopamine D1 receptors in stably cotransfected fibroblast cells. J. Biol. Chem. 273, 4718–4724.
Franco, R., Casadó, V., Ciruela, F., Saura, C., Mallol, J., Canela, E.I., Lluis, C., 1997. Cell surface adenosine deaminase: much more than an ectoenzyme. Prog. Neurosci. 52, 283–294.
Fredholm, B.B., 1995. Adenosine, adenosine receptors and the actions of caffeine. Pharmacol. Toxicol. 76, 93–101.
Ginés, S., Hillion, J., Torvinen, M., Le Crom, S., Casado, V., Canela, E.I., Rondin, S., Lew, J.Y., Watson, S., Zoli, M., Agnati, L., Vernier, P., Lluis, C., Ferré, S., Fuxe, K., Franco, R., 2000. Dopamine D1 and adenosine A1 receptors form functionally interacting heteromeric complexes. Proc. Natl. Acad. Sci. USA 97, 8606–8611.
Kurose, H., Katada, T., Amano, T., Ui, M., 1983. Specific uncoupling by islet-activating protein, pertussis toxin, of negative signal transduction via alpha-adrenergic, cholinergic, and opiate receptors in neuroblastoma×glioma hybrid cells. J. Biol. Chem. 258, 4870–4875.
Latini, S., Bordoni, F., Corradetti, R., Pepeu, G., Pedata, F., 1998. Temporal correlation between adenosine outflow and synaptic potential inhibition in rat hippocampal slices during ischemia-like conditions. Brain Res. 794, 325–328.
Melani, A., Pantoni, L., Corsi, C., Bianchi, L., Monopoli, A., Bertorelli, R., Pepeu, G., Pedata, F., 1999. Striatal outflow of adenosine, excitatory amino acids, GABA and taurine in awake and freely moving rats following middle cerebral artery occlusion: correlations with neurological deficit and histopathological damage. Stroke 30, 2448–2455.
Saura, C.A., Ciruela, F.V., Canela, E.I., Mallol, J., Lluis, C., Franco, R., 1996. Adenosine deaminase interacts with A1 adenosine receptors in pig brain cortical membranes. J. Neurochem. 66, 675–682.
Saura, C.A., Mallol, J., Canela, E.I., Lluis, C., Franco, R., 1998. Adenosine deaminase and A1 adenosine receptors internalize together following agonist-induced receptor desensitization. J. Biol. Chem. 273, 17610–17617.
Wojcik, W.J., Neff, N.H., 1982. Adenosine measurement by a rapid HPLC-fluorometric method: induced changes of adenosine content in regions of rat brain. J. Neurochem. 39, 280–282.

(*Accepted* 31 *January* 2002)

Adenosine A_{2A}-dopamine D_2 receptor-receptor heteromerization. Involvement of epitope-epitope electrostatic interactions.

Francisco Ciruela[1], Javier Burgueño[1], Vicent Casadó[1], Meritxell Canals[1], Daniel Marcellino[1], Steven R. Goldberg[2], Michael Bader[3], Kjell Fuxe[4], Luigi F. Agnati[5], Carmen Lluis[1], Rafael Franco[1], Sergi Ferré[2] and Amina S. Woods[2]*.

[1]Department of Biochemistry and Molecular Biology of the University of Barcelona E-08028, Spain. [2]National Institute on Drug Abuse, Intramural Research Program, NIH, Department of Health and Human Services, Baltimore, MD 21224, USA. [3]Max-Delbrück-Center for Molecular Medicine, D-13092 Berlin-Buch, Germany. [4]Department of Neuroscience, Division of Cellular and Molecular Neurochemistry, Karolinska Institutet, S-171 77 Stockholm, Sweden. [5]Section of Physiology, Department of Biomedical Sciences, University of Modena, 41100 Modena, Italy.

**To whom correspondence should be addressed. Amina S. Woods, National Institute on Drug Abuse, Intramural Research Program, NIH, Department of Health and Human Services, 5500 Nathan Shock Drive, Baltimore, MD 21224. Tel.: 410-550-1507; e-mail: awoods@intra.nida.nih.gov*

ABSTRACT **Previous results from Fluorescence Resonance Energy Transfer (FRET) and Bioluminescence Resonance Energy Transfer (BRET) experiments and computational analysis (docking simulations) have suggested a direct interaction between the N-terminal portion of the third intracellular loop (I3) of the human dopamine D_2 receptor (D2R) and the C-terminal portion of the C-tail from the human adenosine A_{2A} receptor (A_{2A}R). Inspection of the carboxyl terminus of the A_{2A}R revealed the presence of two adjacent aspartic acid residues, which could interact with an Arg-rich region present in the D_2R I3. The peptides corresponding to the relevant epitopes (VLRRRRKRVN in D_2R and HELKGVCPEPPGLDDPLAQDGAVGS in A_{2A}R) do interact, forming non-covalent complexes that were detected by mass spectrometry. *Ab initio* calculations do reinforce, the analytical results. Since the two adjacent Asp present in human A_{2A}R are not conserved among species, another putative epitope for interaction was identified surrounding a serine that can be constitutively phosphorylated in A_{2A}R. A peptide of the phosphorylated epitope (SAQEpSQGNT) formed a non-covalent complex with the D_2R epitope. These results obtained by mass spectrometry were confirmed by using different constructs of the receptors in biochemical pull-down assays. Solubilized D_2R was pulled down by a sepharose-bound GST-fusion protein containing the C-terminal domain of the A_{2A}R. Also, the interaction between wild type A_{2A}R and the Arg-rich peptide of the D_2R was displaced by the two peptides corresponding to the two different sequences in the C-tail of A_{2A}R. In addition, BRET assays confirmed that mutation of Arg residues in the third intracellular loop of D_2R prevents A_{2A}R-D_2R heteromerization. The present results are the first example of epitope-epitope electrostatic interaction underlying receptor heteromerization, a new expanding area of protein-protein interactions.**

Running title: Adenosine A_{2A}-dopamine D_2 receptor-receptor heteromerization
Key words: Functional proteomics, mass spectrometry, BRET, mGlu5 receptor.

INTRODUCTION

The search for better understanding proteins structure-function relationships has ushered the age of proteomics, propelling the study of protein structure to the forefront of research, with the goal of better understanding the role of proteins in the biochemistry, physiology and pathology of the cell, and in finding protein epitopes that play crucial roles in governing cellular interactions. Protein-protein interaction has always played an important role in cellular mechanisms. Often, physiological responses require a group of proteins to interact as exemplified by signaling events such as G proteins cascades. In the past few years it has been shown that G-protein coupled receptors present in the plasma membrane do interact forming functional homomeric or heteromeric receptor complexes.[1-3].

Hence, it is important to understand the mechanisms and chemistry that govern such interactions. Woods et al demonstrated that salt bridge formation occurs between peptides containing two or more adjacent basic residues (e.g. **RR**, **RKR**), and peptides containing two or more adjacent acidic residues (e.g. **EE**, **DD**) or a phosphate group[4-6]. From the results obtained by Canals *et al.*[7] using Fluorescent Resonance Energy Transfer (FRET), Bioluminescence Resonance Energy Transfer (BRET) and computational analysis (docking simulations) it became obvious that an epitope-epitope electrostatic interaction could be the chemical interaction leading to heteromers formation between adenosine A_{2A} receptor (A_{2A}R) and dopamine D_2 receptor (D_2R). These are important receptors for neuronal function and their heteromerization opens new avenues for possible therapeutic approaches for Parkinson's disease and schizophrenia.[2] In this paper a coulombic interaction between a positively charged epitope of the D_2R and a negatively charged epitope of the A_{2A}R was demonstrated by mass spectrometric and pull-down biochemical experiments. The existence of the electrostatic interaction has been confirmed in BRET assays using a mutant version of the D_2R with a lower number of charged amino acids.

METHODS

Peptides Two epitopes from $A_{2A}R$, SAQEpSQGNT (res. 370-378, [MW= 1001.9]) and HELKGVCPEPPGLDDPLAQDGAVGS (res. 388-412 [MW=2500.8]), and one epitope from D_2R, VLRRRRKRVN (res. 215-224 [MW= 1352.7]), as well as VLAAAAAAVN and SAQESQGNT were synthesized at the Johns Hopkins School of Medicine Synthesis and sequencing laboratory. The peptides were diluted in water to a concentration of 10 picomoles/µl for the mass spectrometry experiments.

Mass Spectrometry Mass spectra were acquired in linear mode in both positive and negative ion mode on a DE-PRO MALDI from PE-Biosystems (Framingham, MA), equipped with a nitrogen laser (337 nm) and an extraction voltage of 20 kV. All spectra were the average of 50 shots. Mixtures of the D_2R and each of the $A_{2A}R$ epitopes were prepared. The matrix used, 6-aza-2-thiothymine (ATT) was purchased from Aldrich (Milwaukee, WI), and prepared fresh daily as a saturated solution in 50% ethanol, pH 5.4. No complexes were seen with acidic matrices pH= 1.5. Samples were prepared by adding 0.3 µL peptide mixture to 0.3 µL matrix (ATT) on the sample plate.

Antibodies An antisera against adenosine $A_{2A}R$ was used in this study, designated as anti-CTA2A. This antisera was raised against a GST fusion protein containing aminoacids 322-412 (GST-A2A_{CT}, see below) of the adenosine $A_{2A}R$. The immunization of rabbits and affinity purification of the antisera were performed as described previously.[8,9] The primary antibodies used for immunoblotting were: affinity purified anti-GST polyclonal antibody,[9] polyclonal anti-CTA2A antibody and affinity purified anti-D_2R polyclonal antibody (Chemicon, Temecula, CA, USA). The secondary antibody used was horseradish-peroxidase (HRP)-conjugate goat anti-rabbit (Dako, Denmark).

Cell culture, transfection and membrane preparation HEK-293 cells were grown in DMEM (Sigma Chemical Co., St. Louis, MO, USA) supplemented with 1 mM sodium pyruvate, 2 mM L-glutamine, 100U/ml penicillin/streptomycin, 10% (v/v) foetal bovine serum (FBS) and 0.5 mg/ml of G418 sulphate (GIBCO, Grand Island, NY, USA) at 37ºC and in an atmosphere of 5% CO_2. For the transient expression, cells were transiently transfected with 10 µg of cDNA encoding the human adenosine $A_{2A}R$, human dopamine D_2R, fusion proteins or chimeras by calcium phosphate precipitation.[7,9] The cells were used for experimentation at either 24 or 48 hours after transfection. Cell membranes were obtained by centrifugation after cells disruption with a Polytron homogenizer (Kinematica, PTA 20 TS rotor, setting 4; Brinkmann Instruments, Westbury, NY, USA, three 10-sec periods) in 50 mM phosphate buffer, pH 7.4. Nuclei and cell debris were separated by centrifugation (900 x g, 4ºC). Membranes were pelleted at 105,000 x g (90 min, 4ºC) and resuspended in 50 mM phosphate buffer for immediate use.

Generation and expression of the GST-fusion protein To produce the glutathione S-transferase fusion protein containing the C-terminal domain of adenosine $A_{2A}R$ (GST-A2A_{CT}), the C-terminal tail, amino acids 322-412, of the full length human $A_{2A}R$ in pcDNA3.1 (kindly given by Dr. P. Schofield, The Garvan Institute, Darlinghurst, Sydney, Australia) was amplified with proofreading *Pfu* DNA polymerase and using the primers: FSA2A (5'-TAAGAATTCCGGGTCTTGGCAGCTCATGGC-3') and RA2A (5'-CCGGAATTCCAAGCCAACCAGAAAGAT-AAAG-3'). The EcoRI-EcoRI fragment of the C-Terminal tail of $A_{2A}R$ was subcloned into the bacterial expression vector pGEX-4T-1 (Amersham Biosciences AB, Uppsala, Sweden). The sequence and orientation of the DNA construct was verified by sequencing using ABI Prism BigDye terminator cycle sequencing ready reaction kit (PerkinElmer Life Sciences, Zaventem, Belgium). Recombinant fusion proteins GST and GST-A2A_{CT} were expressed and purified on Glutathione-Sepharose-4B (Amersham Biosciences AB) as described previously.[10] Briefly, bacterial overexpression of GST and GST-A2A_{CT} was facilitated in the *Escherichia coli* BL21 strain (Promega, Madison, WI, USA). The fusion proteins expression was performed with 0.1 mM isopropyl-β-D-thio-galactopyranoside (Sigma Chemical Co., St. Louis, MO, USA) for 3 h at 37 ºC.

Pull-down experiments with the D_2R epitope The D_2R epitope (**VLRRRRKRVN**) corresponding to a region of the third intracellular loop (I3) of the dopamine D_2R, amino acids 215-224, was covalently coupled to EDC (1-Ethyl-3-[3-dimethylaminopropyl]carbodiimide Hydrochloride) (Pierce, Rockford, IL, USA) activated EAH-Sepharose-4B (Amersham Biosciences AB, Uppsala, Sweden) by the carboxy-terminal part. To perform the pull-down experiments of the GST-A2A_{CT} fusion protein the Sepharose-Peptide D_2R was first blocked with blocking buffer (50 mM phosphate buffer, 5 mM EDTA, 0.1% Bovine Serum Albumine, pH 7.4) for 1 h with constant rotation at 4 ºC. After blocking, 50 µl of Sepharose-Peptide D_2R was incubated with GST or GST-A2A_{CT} proteins in blocking buffer for 2 h with constant rotation at 4 ºC. Subsequently, the beads were washed three times with blocking buffer and 60 µl of sodium dodecyl sulfate polyacrylamide gel electrophoresis (SDS-PAGE) sample buffer was added to each sample. GST and GST-A2A_{CT} bound proteins were dissociated by heating to 100ºC for 5 min and resolved by SDS-PAGE. To perform the pull-down experiments of the whole $A_{2A}R$ HEK cells were transiently transfected with human adenosine $A_{2A}R$ and cell membranes, prepared as described above, were solubilized in ice-cold lysis buffer (50 mM phosphate pH 7.4, 1% (v/v) Nonidet P-40) for 30 min at 4 ºC. 50 µl of blocked Sepharose-Peptide D_2R were incubated with the solubilized membranes for 2h with constant rotation at 4 ºC. After incubation, the beads were washed three times with blocking buffer and 60 µl of sodium SDS-PAGE sample buffer was added to each sample. Bound proteins were dissociated by heating at 37 ºC for 1h and resolved by SDS-PAGE.

Pull-down experiments with GST-A2A_{CT} HEK cells were transiently transfected with human D_2R. Cell membranes were solubilized in ice-cold lysis buffer for 30 min at 4 ºC. GST and GST-A2A_{CT} proteins (5 µg each) were coupled to 120µl of a 50% suspension (v/v) of glutathione-agarose beads in phosphate buffer for 1 h with constant rotation at 4 ºC. GST-fusion protein-agarose slurries were preblocked with solubilized membranes of mock transfected cells for 1 h with constant rotation at 4 ºC. Subsequently, the GST-

fusion protein-agarose slurries were incubated with the solubilized membranes of the D_2R transfected cells for 2 h with constant rotation at 4 ºC. After incubation, the beads were washed three times with blocking buffer and 60 µl of sodium SDS-PAGE sample buffer was added to each sample. Bound proteins were dissociated by heating at 37 ºC for 1h and resolved by SDS-PAGE. Sodium dodecyl sulfate polyacrylamide gel electrophoresis (SDS/PAGE) was performed using 10 % polyacrylamide gels. Proteins were immunoblotted to PVDF membranes (Immobilon-P, Millipore, Watford, U.K.) using a semidry transfer system and developed with the enhanced chemiluminescence detection kit (Pierce), as described previously.[8]

BRET experiments using mutant D_2R Detailed expression vectors and transfections are given in detail elsewhere.[7] HEK293 cells were transfected with wild type or mutant human D_2R. Mutant D_2R consists of a change of 5 amino acids, from 416LRRRR420 in the wild type to 416AQKQI420 in the mutant. For BRET assays, HEK293 cells, forty-eight hours post-transfection, were rapidly washed twice in PBS, detached, and resuspended in the same buffer. To control the number of cells, samples protein concentration was determined using a Bradford assay kit (Bio-Rad, Munich, Germany) using BSA dilutions as a standard. To quantify $A_{2A}R$-Rluc and D_2-YFP expression, cell suspension (20 µg of protein) was distributed in duplicate into 96-well microplates (Corning #3604, U.S.A, white plates with transparent bottom). The fluorescence was measured using a Packard FluoroCount™ with an excitation filter of 485nm and an emission filter of 530nm using the following parameters: Gain of 1, PMT fixed at 1100V, and read time of 1 s. Fluorescence was quantified as an in-fold over the background (mock transfected cells). The same samples were incubated for 10 min with 5µM coelenterazine H (Molecular Probes, Eugene, OR, U.S.A) and the luminescence was measured using a Packard LumiCount™ with the following parameters: Gain of 1, PMT fixed at 700V, and a read time of 1 s. For BRET measurement, 20 µg of cell suspension were distributed in duplicates in 96-well microplates (Corning #3600, U.S.A white opaque plates) and 5 µM coelenterazine H was added. After 1 minute the readings were collected by using a Fusion microplate analyzer (Packard, Meriden, CT) that allows the integration of the signals detected in the 485 and the 530nm windows using filters with the appropriate band pass. The BRET ratio is defined as [(emission at 510-590) - (emission 440-500) x Cf] / (emission at 440-500) where Cf corresponds to (emission at 510-590) / (emission at 440-500) for the -Rluc construct expressed alone in the same experiment.

ERK phosphorylation assays Transfected HEK293 cells were grown to 80% confluence and rendered quiescent by serum starvation overnight prior to MAPK phosphorylation assays, an additional 2h incubation in fresh serum-free medium was performed to minimize basal activity. Cells were subsequently stimulated by addition of medium with or without the D_2R agonist quinpirole or the D_2R antagonist raclopride. Stimulation was terminated by rinsing rapidly with ice-cold PBS and cell lysis was performed by the addition of 500 µl of ice-cold lysis buffer (50 mM Tris-HCl pH 7.4, 50 mM NaF, 150 mM NaCl, 40 mM B-Glycerophosphate, 1% Triton 100X, 20 µM phenyl-arsin oxide, 1mM $NaVO_4$ and protease inhibitor cocktail). The cellular debris was removed by centrifugation at 13000xg for 5 min, and the total protein content was measured using BCA Protein Assay Reagent (Pierce). Aliquots corresponding to 5µg of protein were mixed with SDS loading buffer, applied to 7.5% SDS-Polyacrylamide gel electrophoresis and analyzed by Western blot. ERK1/2 activation was assayed by incubating PVDF blots with a mouse anti-phospho-ERK1/2 antibody (Sigma, 1:10000); in order to rule out that the differences observed were due to the application of unequal amounts of lysates, control blots were also run in parallel and proved with a rabbit anti-ERK1/2 antibody that recognizes both, unphosphorylated and phosphorylated forms (Sigma, 1:40000). The immunoreactive bands were visualized using horseradish peroxidase linked secondary anti-mouse and anti-rabbit antibodies (DAKO) and SuperSignal West Pico Chemiluminescent Substrate (Pierce).

Confocal microscope observations Transfected HEK-293T cells were fixed in 4% paraformaldehyde for 15 min and washed with PBS containing 20 mM glycine (buffer A) to quench the aldehyde groups. Confocal microscope observations were made with a Leica TCS-SPII (Leica Lasertechnik, Heidelberg, Germany) confocal scanning laser microscope adapted to an inverted Leitz DMIRBE microscope with excitation of the YFP protein fused to the D_2R mutant at 514 nm.

Table 1. Interspecies comparison of the $A_{2A}R$ and D_2R epitopes

From	Sequence	res #	Accession #
Human	SAQEpSQGNT	370-378	P29274
Guinea Pig	SAQRpSGDAS	367-376	P46616
Rat	SAQGpSPRDV	365-373	P30543
Mouse	STQGpSPGDV	365-373	Q60613
Dog	IAPEpSHGDM	370-378	P11617
Human	HEL KGVCPEPPGL DDPLAQDGAG VS	388-412	P29274
G. pig	HEHKGTCPESPSLEDPPAHGGAGVS	385-409	P46616
Mouse	HPGLG DHLAQGRVGTASWSSEFAPS	386-410	Q60613
Rat	HPGLR GHLVQARVGASSWSSEFAPS	386-410	P30543
Dog	HEL KGACPESPGLEGPLAQDGAG VS	388-412	P11617
Human	VLRRRRKRVN	215-224	P14416
Green Monkey	VLRRRRKRVN	215-224	P52702
Bovine	VLRRRRKRVN	215-224	P20288
Mouse	VLRKRRKRVN	215-224	P13953
Rat	VLRRRRKRVN	215-224	NM012547
Turkey	VLRKRRKRVN	215-224	O73810
Frog	VLRKRRKRVN	208-218	P24628

RESULTS

Mass Spectrometry

According to the modeling results of $A_{2A}R$-D_2R heterodimerization given by Canals *et al*.,[7] the positively charged Arg residues in the I3 of the D_2R did interact with the negatively charged residues in the C-tail of $A_{2A}R$. A visual inspection of the human $A_{2A}R$ sequence (accession # P29274) indicates the presence of adjacent Asp residues **DD**$_{401\text{-}402}$ in the epitope: **HELKGVCPEPPGLDDPLAQDGAVGS**. Mixtures with equal volumes of the peptide **VLRRRRKRVN** containing 6 adjacent basic residues **RRRRKR**$_{217\text{-}222}$, corresponding to the epitope from the I3 of the human D_2R sequence (accession # P 13953) and peptide **HELKGVCPEPPGLDDPLAQDGAVGS** corresponding to the epitope from the carboxyl terminus of the human $A_{2A}R$ were prepared and analyzed by mass spectrometry. Spectra were acquired and showed the following molecular ions (MH^+): 1353.7 and 2501.8 for each epitope and 3854.5 for the complex (Figure 1), confirming the likelihood of a Coulombic interaction between these two peptides. No complexes formed between either $A_{2A}R$ epitopes and **VLAAAAAAVN**, or **SAQESQGNT** and **VLRRRRKRVN.**

The two adjacent negatively charged **DD** residues present in the human $A_{2A}R$ sequence are only conserved in guinea pig but not in other species such as mouse, rat or dog (table I). The perusal of the Swiss Prot and Entrez databases showed that a serine, which is susceptible to constitutive phosphorylation, is conserved among various species (table 1). A phosphorylated serine residue in the Carboxyl terminus of the $A_{2A}R$ could also be a candidate for interaction with the third intracellular loop of D_2R in heteromer formation. To check this possibility, mixtures containing equal volumes of peptide **VLRRRRKRVN** corresponding to the epitope of the human D_2R and the phosphorylated epitope **SAQEpSQGNT** corresponding to the phosphorylated serine version of the epitope of the human $A_{2A}R$ were prepared and analyzed by mass spectrometry. Spectra were acquired and showed the following molecular ions (MH^+): 1353.7 and 1001.9 for each epitope and 2354.6 for the complex (Figure 2), thus confirming that the Args from the D_2R epitope can also interact with the phosphorylated epitope from $A_{2A}R$. Hence, the mass spectrometry data supports the possible involvement of one or both epitopes in the cytoplasmic Carboxyl terminal domain of the adenosine $A_{2A}R$ receptor in its interaction with a positively charged epitope of the third intracellular loop of the dopamine D_2R.

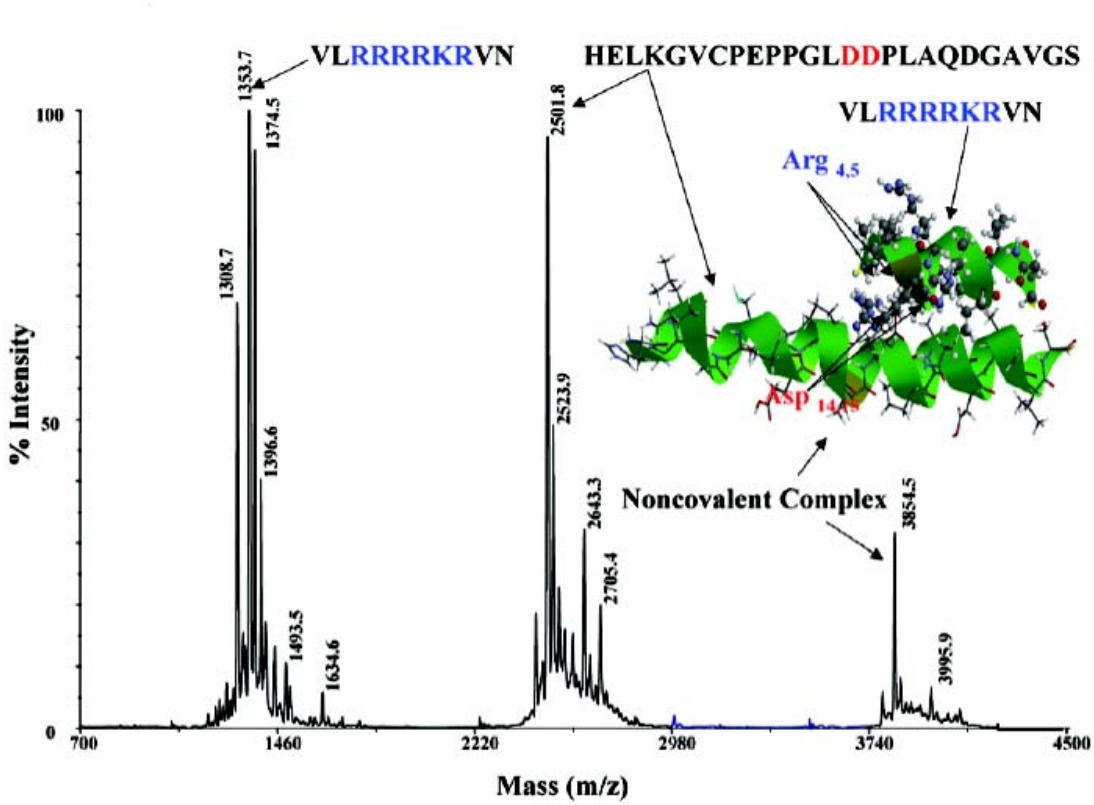

Figure 1: Mass spectrum of a mixture of $A_{2A}R$ and D_2R epitopes. The mixture of HELKGVCPEPPGLDDPLAQDGAVGS and VLRRRRKRVN resulted in the formation of a noncovalent complex seen at m/z 3854.5 amu. The spectrum was acquired in positive ion mode using ATT as a matrix. The insert shows the electrostatic potential modeling of the epitopes.

***Ab Initio* Calculations**

Geometry optimization of all peptides was carried out at the Hartree-Fock 6-31G** level of theory using Spartan '02 (Wavefunction, Inc., Irvine, CA). The plot of the electrostatic potential surface of peptides **HELKGVCPEPPGLDDPLAQDGAVGS** and **VLRRRRKRVN** is shown in Figure 1, and that of peptides **SAQEpSQGNT** and **VLRRRRKRVN** is seen in Figure 2. The Electrostatic potential surfaces were generated by mapping the 6-31G** electrostatic potentials. Briefly, red colors represent regions of negative potential while blue colors represent areas of positive potential. Orange, yellow, green and light green represent regions of intermediate potential. Guanidinium groups are blue, and carboxyl groups and phosphate are red. Calculations for each molecule were done separately.

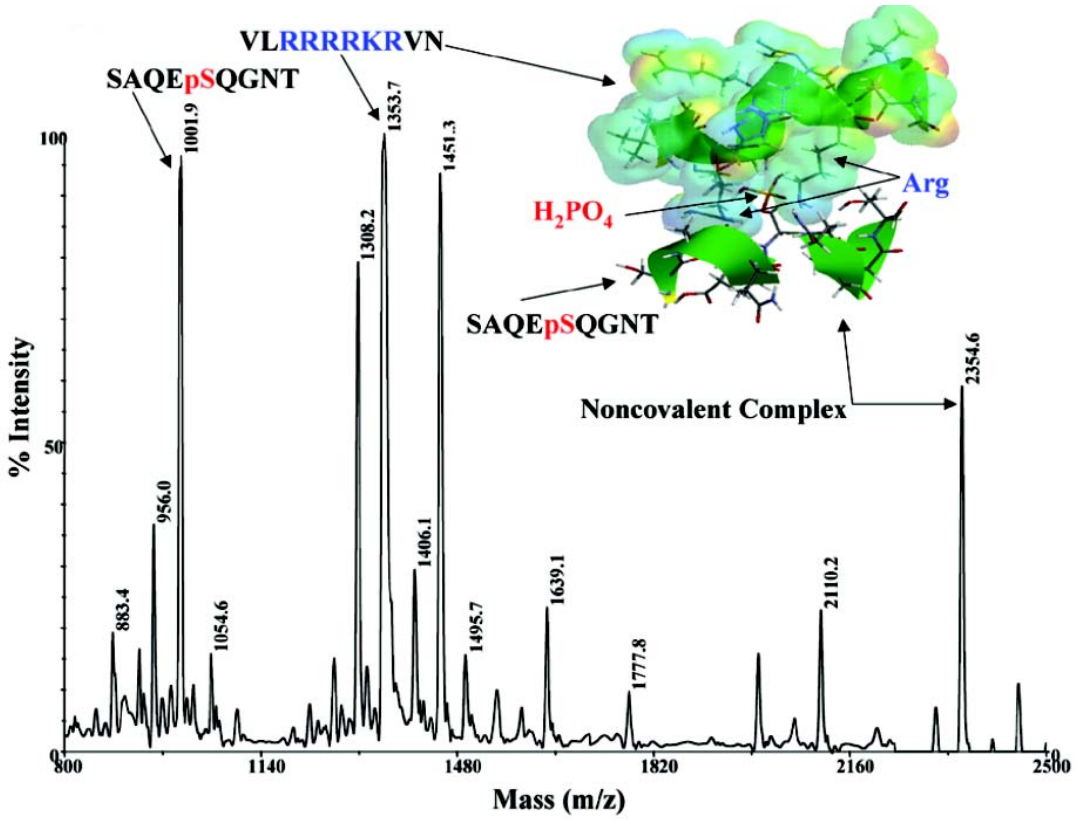

Figure 2: Mass spectrum of a mixture of $A_{2A}R$ and D_2R epitopes. The mixture of **SAQEpSQGNT** and **VLRRRRKRVN** resulted in the formation of a noncovalent complex seen at m/z 2354.6 amu. The spectrum was acquired in positive ion mode using ATT as a matrix. The insert shows the electrostatic potential modeling of the epitopes.

Pull-down of the C-terminal $A_{2A}R$ with the D_2R epitope

A GST-fusion protein containing the C-terminal domain of the $A_{2A}R$ receptor (GST-A2A$_{CT}$) (Fig. 3A) and the **RRRRKR**-containing epitope of the N-terminal portion of the I3 of the D_2R (sepharose bound) were used (Fig. 3B). The fusion protein contains the last 91 amino acids of the cytoplasmic C-terminal tail of the adenosine $A_{2A}R$ (Fig. 3A), which has an isolectric point of 4.8 and a charge at pH 7.0 of minus 5.4. On the other hand, the D_2R epitope contains 6 adjacent basic amino acids, has an isolectric point of 12.7 and a charge at pH 7.0 of plus 5.9. These parameters support the likelihood of a Coulombic interaction between these two epitopes.

Incubation of the D_2R epitope with GST or GST-A2A$_{CT}$ resulted in the pull down of GST-A2A$_{CT}$ only (Fig 3C) as detected in the Western blot using an antibody to GST, thus confirming the interaction of D_2R epitope with an epitope on C-terminal tail of $A_{2A}R$ (Fig. 3C). Interestingly, this interaction is also concentration-dependent and the binding is saturable (Fig. 3D). Under these experimental conditions, the equilibrium binding studies[11] gave an apparent K_D of 2±0.2 nM.

Pull-down of the D_2R with the C-terminal $A_{2A}R$

GST or GST-A2A$_{CT}$ were sepharose bound and a solubilized D_2R was added. An antibody to D_2R is used in the Western blot, and as seen in Figure 4, D_2R is only detected in the GST-A2A$_{CT}$ lane and not in the GST lane, thus confirming that an epitope in the C-terminal domain of $A_{2A}R$ binds to the complete D_2R molecule.

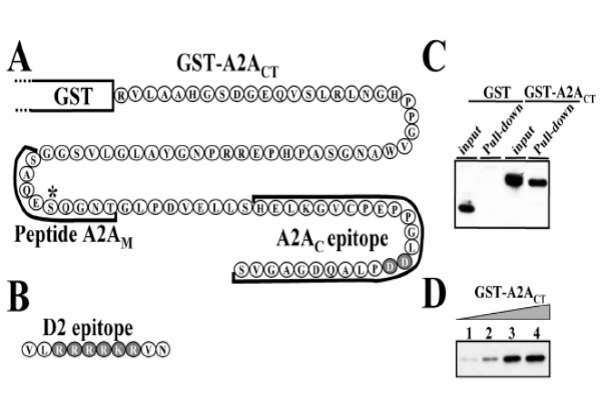

Figure 3
Interaction of GST-A2ACT with D2R epitope. **Panel A.** Schematic representation of the GST-A2ACT fusion protein. The underlined sequence corresponds to the two A2AR epitopes. The residue marked with an asterisk represents the phosphorylated serine. **Panel B.** Amino acid sequence of the epitope found in the third intracellular loop of the D2R. The gray shaded residues represent the positively charged amino acids. **Panel C.**
GST and GST-A2ACT pull-down experiment. 50 ng of GST or GST-A2ACT proteins (see input) were incubated with the D2R epitope coupled to Sepharose-4B. After the pull-down experiment (see Experimental Procedures), proteins bound to the D2R-epitope were dissociated and resolved by SDS-PAGE in 10% gels and immunoblotted using a polyclonal anti-GST antibody (1/200). The primary bound antibody was detected using a goat anti-rabbit antibody. **Panel D.** Association of the GST-A2ACT to the D2R epitope. Increasing concentrations of the GST-A2ACT (lane 1: 5 ng; lane 2: 10 ng; lane 3: 50 ng; lane 4: 100 ng) were incubated with Sepharose-D2R epitope. After the pull-down experiment, protein bound to the Sepharose-D2R epitope was dissociated and resolved by SDS-PAGE in 10% gels and immunoblotted using a polyclonal anti-GST antibody (1/200). The primary bound antibody was detected using a goat anti-rabbit antibody.

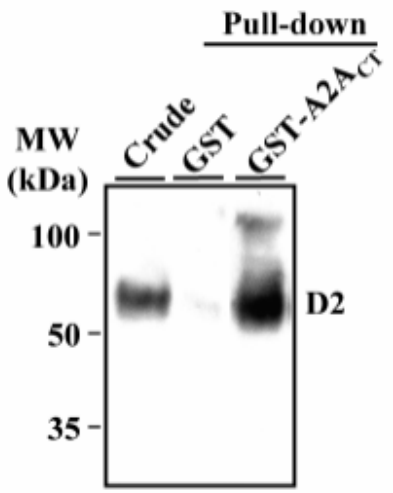

Figure 4 Interaction of D2R with GST-A2ACT. Transiently transfected HEK cells with D2R were solubilized in lysis buffer. The solubilized proteins (Crude) were incubated with Agarose-glutathione-GST or Agarose-glutathione-GST-A2ACT. After the pull-down experiment (see Experimental Procedures), proteins bound to the Agarose-glutathione-GST or Agarose-glutathione-GST-A2ACT were resolved by SDS-PAGE and immunoblotted using a polyclonal anti-D2R antibody (2 mg/ml). The primary bound antibody was detected using a goat anti-rabbit antibody.

Pull-down of the Adenosine A_{2A}R with the D_2R epitope

Two immunoreactive bands, 40kDa and 80kDa, for the adenosine A_{2A}R monomer and dimer, were detected in the crude extract from HEK-293 cells transiently transfected with adenosine A_{2A}R (Fig. 5A, Crude). The two bands were only detected in pull-down assays when cell lysates were incubated with the D_2R epitope (sepharose bound), but were not seen with sepharose alone (Fig. 5A, Pull-down). This result confirms that the adenosine A_{2A}R receptor binds to a region of the I3 of the D_2R. This interaction was displaced by the epitope containing the 25 terminal residues of adenosine A_{2A}R, (Fig. 5B), which supports a role of this A_{2A}R epitope in the interactions with the D_2R (Fig. 5B). When a similar experiment was conducted using the nine amino acid long epitope belonging to the C-terminal tail of the A_{2A}R **SAQESQGNT** (Fig. 5A) where the Ser residue is not phosphorylated, no displacement occurred. This peptide has only one acidic amino acid (E), an isolectric point of 3.7 and a charge at pH 7.0 of –1, so the weak interaction with the D_2R epitope is not surprising. However when the same epitope is phosphorylated at residue 374 **SAQEpSQGNT**, thus increasing its negative charge (Phosphate has a pKa of 2.2), a displacement was observed in the pull-down experiment (Fig. 5A). This result suggests a potential role for the phosphorylation / dephosphorylation events in the A_{2A}R-D_2R direct interaction.

BRET saturation curve for A_{2A}R-Rluc and D_2R-YFP or mutant D_2R-YFP

BRET measurements were performed in transiently co-transfected HEK-293T cells using a constant amount of A_{2A}R-Rluc and increasing amounts of either wild type D_2R-YFP (416LRRRR420), or mutant D_2R-YFP (416AQKQI420). Fluorescence levels were checked by independent measurements and normalized to the level of luciferase detected per sample (fluorescence in arbitrary units). As indicated in Figure 6, BRET is markedly reduced when the mutant receptor is used in the assays. This further confirms that adjacent Arg residues in the third intracellular loop of the D_2R are crucial for A_{2A}R/D_2R heteromerization. Membrane expression and functionality of the D_2R was confirmed by Western blotting, confocal microscopy and ERK1/2 activation (Figure 7). Both receptors showed ERK1/2 activation with the D_2R agonist quinpirole, which was counteracted with the D_2R antagonist raclopride.

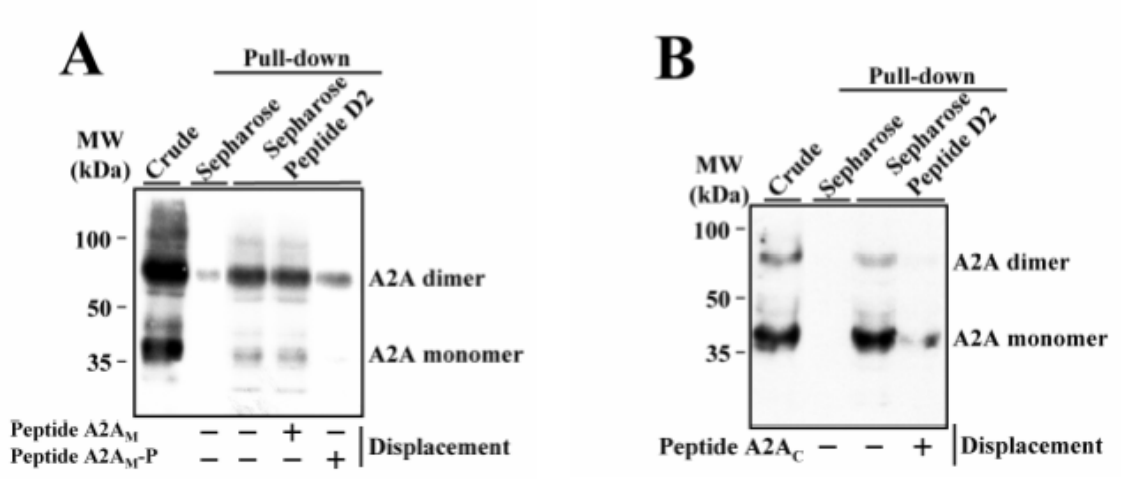

Figure 5 Interaction of the $A_{2A}R$ receptor with the D_2R epitope. Panel A. Transiently transfected HEK cells with $A_{2A}R$ were solubilized in lysis buffer. The solubilized proteins (Crude) were incubated with Sepharose or with Sepharose-D_2R epitope in the presence or absence of the non-phosphorylated or phosphorylated $A_{2A}R$ receptor epitope SAQESQGNT (2 mM) or SAQEpSQGNT (2 mM), respectively. After the pull-down experiment (see Experimental Procedures), proteins bound to the Sepharose or Sepharose-D_2R epitope were resolved by SDS-PAGE and immunoblotted using a polyclonal anti-CTA2A antibody (1/2000). The primary bound antibody was detected using a goat anti-rabbit antibody. Displacement was only observed with the phosphorylated $A_{2A}R$ epitope. Panel B. the same experiment as in panel A was conducted using the epitope containing the 25 terminal residues of adenosine $A_{2A}R$, and showed displacement.

DISCUSSION

A gradual accumulation of data on receptor-receptor interaction at the plasma membrane level has taken place over the past few years. Receptors have been involved in influencing each other's way of decoding their respective first messenger.[1-3] Two main models have been suggested for the formation of receptor G-protein coupled receptor homo- or heterodimers: the "domain swapping" and the "domain contact".[12,13] Both interactions can also occur simultaneously, thus allowing the formation of high-order hetero-oligomers. The prevalence of one of the two models may depend on the receptor type and on the chemical-physical environments in which the interacting receptors are embedded. Gouldson and colleagues have used molecular dynamics simulations to evaluate the energy of different dimer formation models for adrenergic receptors. It has been shown that the 5-6 transmembrane domain swapped dimer is a high-energy structure both in the absence of ligands and in the presence of antagonist.[13] For other G-protein coupled receptors, however, other domains seem to be involved. In the case of the $GABA_B$ receptors, a coiled coil interaction between C terminal domains is implicated in $GABA_BR1$-$GABA_BR2$ heterodimerization,[14] while in the case of metabotropic glutamate receptors disulphide bridges in the extracellular portion are responsible for homodimerization.[15] The existence of $A_{2A}R$-D_2R heteromeric complexes was previously demonstrated by coimmunoprecipitation experiments performed on membrane preparation of D_2R-transfected SH-SY5Y neuroblastoma cells.[16] Canals *et al.*[7] have provided evidence for a direct protein-protein interaction between both receptors by using FRET and BRET techniques. The results described in this study are not only crucial for understanding the molecular mechanisms which are involved in $A_{2A}R$-D_2R heterodimerization, they are also the first example of epitope-epitope electrostatic interaction underlying receptor heteromerization, a new expanding area of protein-protein interactions.[1-3]

In order to strengthen our hypothesis on $A_{2A}R$-D_2R heteromerization,[7] we studied and compared sequences from different sources, to find candidate epitopes, on both $A_{2A}R$ and D_2R, that could participate in an electrostatic interaction. Our data not only support the direct $A_{2A}R$-D_2R interaction, they also give insights on the epitopes involved in the interaction. Both the mass spectometry and pull-down data show that two different epitopes in the C-terminal part of the $A_{2A}R$ can bind directly to a D_2R epitope situated in the N-terminal part of the third intracellular loop (I3). The residues participating in this interaction have opposite charges, thus allowing the formation of a salt bridge between the epitopes involved. On the $A_{2A}R$ carboxyl terminus one of the epitopes has two adjacent Asp residues, whereas the other epitope corresponds to a sequence containing a Ser residue with a strong likelihood of being phosphorylated. The highly negatively charged phosphate group on this Ser would mediate the interaction with D_2R I3. The positively charged epitope present in the D_2R I3 has six adjacent basic residues, five of which are Arg. In the side chain of Arg, the functional group is a guanidinium composed of three nitrogens and a central carbon, each contributing one π orbital, thus producing one bonding and two non-bonding molecular orbitals and a fourth antibonding orbital. The guanidium cation has six π electrons distributed in pairs among the three molecular orbitals. The two highest occupied non-bonding molecular orbitals are degenerate in energy and distribute two pairs of electrons evenly over the three nitrogen atoms, resulting in equal sharing of the one

positive formal charge among the three nitrogens, thus making Arg the most basic amino acid residue. The guanidium group defines the plane in which the central carbon, three nitrogens, five hydrogens and the δ-carbon reside. The hydrogens bristle from the three nitrogens at 120° angles around the periphery and the flat cloud of π electrons sandwich the σ structure from above and below. The structure has a net positive charge that can be neutralized by removing a proton, which is what happens when it interacts with a phosphate group or adjacent acidic residues, which have a delocalized lone pair of electrons on the phosphate or the side chain carboxyl group.[17]

The Ser susceptible of phosphorylation in the C-tail sequence of $A_{2A}R$ is in an epitope having a casein-kinase I consensus site (**SAQEpS**). Comparison of the sequences from rat, mouse and human shows that the two adjacent Asp are not conserved among species whereas the casein-kinase I consensus site is present in all the sequences. Since there is indirect evidence of $A_{2A}R$-D_2R heteromerization in the rat striatum,[18] it is likely that the heterodimerization is mediated by the phosphorylated epitope. Whether the second epitope present in human (and in guinea pig) is a redundant mechanism in human $A_{2A}R$-D_2R heterodimerization remains to be determined. Our data also suggest that neurotransmitter or neuromodulator-mediated phosphorylation-dephosphorylation events could regulate receptor-receptor heteromerization. Activation of $A_{2A}R$, D_2R or both, has no effect on $A_{2A}R$-D_2R heterodimerization.[7] Therefore, activation cascades triggered by adenosine or dopamine through $A_{2A}R$-D_2R heteromers do not seem to affect the degree of phosporylation of the **SAQEpS** epitope. Greengard's group has recently demonstrated that caseine-kinase I activity is regulated by group I metabotropic glutamate receptors.[19] In the striatum $A_{2A}R$ are not only colocalized with D_2R, but also form functional heteromeric receptor complexes with group I metabotropic glutamate receptors $mGlu_5$ ($mGlu_5R$).[20] $A_{2A}R$ and $mGlu_5R$ interact synergistically at different levels[2,20-24] and, in fact, $mGlu_5R$ stimulation potentiates the antagonistic intramembrane $A_{2A}R$-D_2R interaction.[21,22] Therefore, a casein-kinase I- mediated phosphorylation of $A_{2A}R$ could be a possible mechanism by which mGlu5R could modulate $A_{2A}R$-D_2R heteromerization. In addition according to Chothia and Janin[25] when protein subunits interact *in vivo* they form a stable non-covalent bond by neutralizing each other's charge. However when they separate, the cell's aqueous medium, provides ions, such as electrolytes, from the cell milieu to interact with the protein molecules, to neutralize their charge. When control epitopes were used, when the positive charge of Arg was replaced by the neutral Ala or the negative charge of the phosphorylated Ser was replaced by a non-phosphorylated residue, the interaction did not take place.

Two isoforms of D_2R ($D_{2L}R$ and $D_{2S}R$) are generated by alternative splicing and $D_{2L}R$, which was the isoform of the D_2R used in the present experiments (pull-down and BRET), contains 29 additional amino acid residues within the middle portion of the I3. However, the D_2R epitope that binds to the $A_{2A}R$ is localized in the N-terminal portion of the long I3, and is therefore, common to both D_2R isoforms. This arginine-rich D_2R region has also been shown to bind to other proteins, such as filamin-A and protein 4.1N, which are cytoskeletal-associated proteins.[26,27] These interactions may be important for establishing the correct subcellular localization of D_2R. The arginine-rich D_2R epitope is also present in other proteins. Hence, our suggestion that this epitope could be relevant to a number of additional protein-protein interactions. An attractive hypothesis would be that this epitope, if present in different proteins, could serve to establish dynamic interactions, which would probably depend on the density and strength of the interaction with its possible partners.

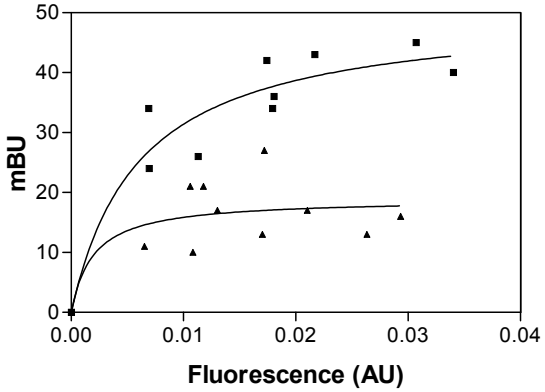

Figure 6
BRET saturation curve for A2AR luc-D2R YFP and D2R mutant YFP. BRET measurements were performed in transiently co-transfected HEK-293T cells using a constant amount of A2AR-Rluc and increasing amounts of either D2R-YFP (containing the epitope **VLRRRRKRVN**; squares), or mutant D2R-YFP (containing the epitope **VLAQKQIRVN**; triangles). BRET is markedly reduced when the mutant receptor is used in the assays. AU: arbitrary units; mBU: mBRET units.

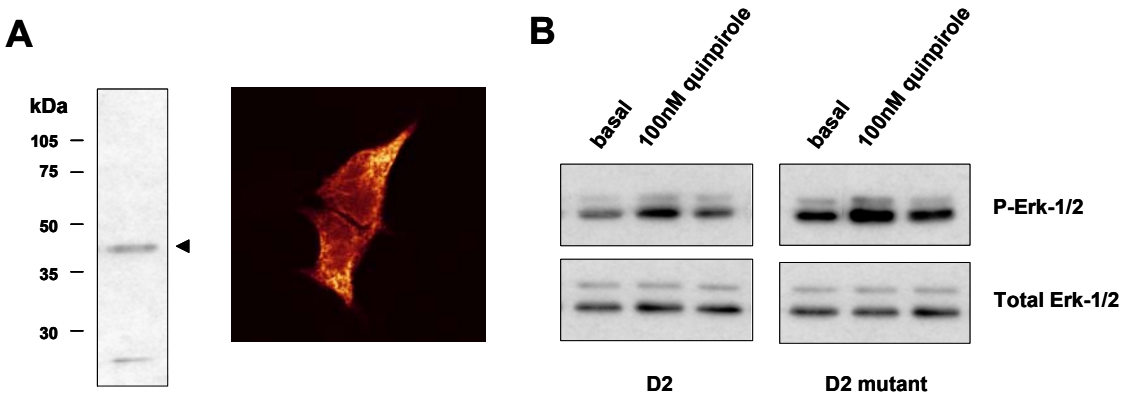

Figure 7 Expression and functionality tests of the D_2R mutant YFP. A. Membrane expression of the D_2R mutant YFP receptor in HEK-293T cells transiently transfected with the cDNA corresponding to the D_2R mutant YFP was evaluated by both Western blot and confocal microscopy. B. D_2R and D_2R mutant transfected cells were treated with the D_2R agonist quinpirole or with quinpirole + the D_2R antagonist raclopride for 10 min at 37ºC and ERK-1/2 phosphorylation. Both receptors were functional and showed ERK1/2 activation with quinpirole, which was counteracted with raclopride.

AGNOWLEDGEMENTS

This work was supported by the European Union (QLG3-CT-2001-010566), Ministerio de Ciencia y Tecnología (SAF2002-03293 and SAF2001-3474), Fundacio la Caixa (02/056-00) and Fundació Marató of Catalonian Telethon (01/012710). We thank Drs. Roy Wise and Barry Hoffer for their intellectual and financial support.

REFERENCES

1. Bouvier M. Oligomerization of G-protein-coupled transmitter receptors. Nat Rev Neurosci 2001;2:274-286.
2. Agnati LF, Ferré S, Lluis C, Franco R, Fuxe K. Molecular mechanisms and therapeutical implications of intramembrane receptor/receptor interactions among heptahelical receptors with examples from the striatopallidal GABA neurons. Pharmacol Rev 2003;55:509-550.
3. Franco R, Canals M, Marcellino D, Ferré S, Agnati LF, Mallol J, Casadó V, Ciruela F, Fuxe K, Lluis C, Canela EI. Regulation of heptaspanning-membrane-receptor function by dimerization and clustering. Trends Biochem Sci 2003;28:238-243.
4. Woods AS, Huestis MA. A study of peptide--peptide interaction by matrix-assisted laser desorption/ionization. J Am Soc Mass Spectrom 2001;12:88-96.
5. Woods AS, Koomen J, Ruotolo B, Gillig KJ, Russell DH, Fuhrer K, Gonin M, Egan T, Schultz JA. A study of peptide-peptide interactions using MALDI ion mobility o-TOF and ESI mass spectrometry. J Am Soc Mass Spectrom 2002;13:166-169.
6. Woods AS, Moyer SC, Wang HYJ, Wise RA. Interaction of chlorisondamine with the neuronal nicotinic acetylcholine receptor. J Proteome Res 2003;2:207-212.
7. Canals M, Marcellino M, Fanelli F, Ciruela F, de Benedetti P, Goldberg S, Fuxe K, Agnati LF, Woods AS, Ferré S, Lluis C, Bouvier M, Franco R. Adenosine A2A-dopamine D2 receptor-receptor heteromerization. Qualitative and quantitative assessment by fluorescence and bioluminescence energy transfer. J Biol Chem (in press).
8. Ciruela F, McIlhinney RAJ. Differential internalisation of mGluR1 splice variants in response to agonist and phorbol esters in permanently transfected BHK cells. FEBS Lett 24;418:83-86.
9. Clark RAC, Gurd JW, Bisson N, Tricaud N, Molnar E, Zamze SE, Dwek RA, McIlhinney RAJ, Wing DR. Identification of lectin-purified neural glycoproteins, GPs 180, 116, and 110, with NMDA and AMPA receptor subunits: conservation of glycosylation at the synapse. J Neurochem 1998;70:2594-2605.
10. Jordan M, Schallhorn A, Wurm FM. Transfecting mammalian cells: optimization of critical parameters affecting calcium-phosphate precipitate formation. Nucleic Acids Res 1996;24:596-601.
11. Casado V, Canti C, Mallol J, Canela EI, Lluis C, Franco R. Solubilization of A1 adenosine receptor from pig brain: characterization and evidence of the role of the cell membrane on the coexistence of high- and low-affinity states. J Neurosci Res 1990;26:461-473.
12. Gouldson PR, Snell CR, Bywater RP, Higgs C, Reynolds CA. Domain swapping in G-protein coupled receptor dimers. Protein Eng 2001;14:759-767.
13. Gouldson PR, Higgs C, Smith RE, Dean MK, Gkoutos GV, Reynolds CA. Dimerization and domain swapping in G-protein-coupled receptors:

a computational study. Neuropsychopharmacology 2000;23:S60-S77.
14. Pagano A, Rovelli G, Mosbacher J, Lohmann T, Duthey B, Stauffer D, Ristig D, Schuler V, Meigel I, Lampert C, Stein T, Prezeau L, Blahos J, Pin J, Froestl W, Kuhn R, Heid J, Kaupmann K, Bettler B. C-terminal interaction is essential for surface trafficking but not for heteromeric assembly of GABA(b) receptors. J Neurosci 2001;21:1189-1202.
15. Robbins MJ, Ciruela F, Rhodes A, McIlhinney RA. Characterization of the dimerization of metabotropic glutamate receptors using an N-terminal truncation of mGluR1alpha. J Neurochem 1999;72:2539-2547.
16. Hillion J, Canals M, Torvinen M, Casado V, Scott R, Terasmaa A, Hansson A, Watson S, Olah ME, Mallol J, Canela EI, Zoli M, Agnati LF, Ibanez CF, Lluis C, Franco R, Ferré S., Fuxe, K. Coaggregation, cointernalization, and codesensitization of adenosine A2A receptors and dopamine D2 receptors. J Biol Chem 2002;277:18091-18097.
17. Kyte J. Structure in Protein Chemistry.New-York: Garland Publishing, Inc.; 1995.
18. Ferré S, von Euler G, Johansson B, Fredholm BB, Fuxe K. Stimulation of high-affinity adenosine A2 receptors decreases the affinity of dopamine D2 receptors in rat striatal membranes. Proc Natl Acad Sci U S A 1991;88:7238-7241.
19. Liu F, Virshup DM, Nairn AC, Greengard P. Mechanism of regulation of casein kinase I activity by group I metabotropic glutamate receptors. J Biol Chem 2002;277:45393-45399.
20. Ferré S, Karcz-Kubicha M, Hope BT, Popoli P, Burgueno J, Gutierrez MA, Casado V, Fuxe K, Goldberg SR, Lluis C, Franco R, Ciruela F. Synergistic interaction between adenosine A2A and glutamate mGlu5 receptors: implications for striatal neuronal function. Proc Natl Acad Sci U S A 2002;99:11940-11945.
21. Ferré S, Popoli P, Rimondini R, Reggio R, Kehr J, Fuxe K. Adenosine A2A and group I metabotropic glutamate receptors synergistically modulate the binding characteristics of dopamine D2 receptors in the rat striatum. Neuropharmacology 1999;38:129-140.
22. Popoli P, Pezzola A, Torvinen M, Reggio R, Pintor A, Scarchilli L, Fuxe K, Ferré S. The selective mGlu(5) receptor agonist CHPG inhibits quinpirole-induced turning in 6-hydroxydopamine-lesioned rats and modulates the binding characteristics of dopamine D(2) receptors in the rat striatum: interactions with adenosine A(2a) receptors. Neuropsychopharmacology 2001;25:505-513.
23. Ferré S, Ciruela F, Woods AS, Canals M, Burgueno J, Marcellino D, Karcz-Kubicha, M, Hope BT, Morales M, Popoli P, Goldberg SR, Fuxe K, Lluis C, Franco R, Agmati LF. Glutamate mGlu5-adenosine A2A-dopamine D2 receptor interactions in the striatum. Implications for drug therapy in neuropsychiatric disorders and drug abuse. Curr Med Chem-Central Nervous Systems Agents 2003;33:1-26.
24. Nishi A, Liu F, Matsuyama S, Hamada M, Higashi H, Nairn AC, Greengard P Metabotropic mGlu5 receptors regulate adenosine A2A receptor signaling. Proc Natl Acad Sci U S A 2003;100:1322-1327.
25. Chothia C, Janin J. Principles of protein-protein recognition. Nature 1975;256:705-708.
26. Lin R, Karpa K, Kabbani N, Goldman-Rakic P, Levenson R. Dopamine D2 and D3 receptors are linked to the actin cytoskeleton via interaction with filamin A. Proc Natl Acad Sci U S A 2001;98:5258-5263.
27. Binda AV, Kabbani N, Lin R, Levenson R. D2 and D3 dopamine receptor cell surface localization mediated by interaction with protein 4.1N. Mol Pharmacol 2002;62:507-513.